January 2015

Topographical Enhancement of Cell Adhesion on Poorly Adhesive Materials

Maritza Muniz Maisonet
University of South Florida, munizet@gmail.com

Topographical Enhancement of Cell Adhesion on Poorly Adhesive Materials

by

Maritza Muñiz Maisonet

A dissertation submitted in partial fulfillment
of the requirements for the degree of
Doctor of Philosophy in Chemical Engineering
Department of Chemical and Biomedical Engineering
College of Engineering
University of South Florida

Co-Major Professor: Ryan G. Toomey, Ph.D.
Co-Major Professor: Nathan D. Gallant, Ph.D.
John M. Wiencek, Ph.D.
Mark Jaroszeski, Ph.D.
Garrett Matthews, Ph.D.

Date of Approval:
July 23, 2015

Keywords: Topography, Electrospun Fibers,
PNIPAAm, Biomaterials, Cell Attachment

DEDICATION

I dedicate this dissertation to my family for their dedicated love and support throughout this journey, without them this would not have been a possibility, in special, to my mom for always believing in me and for not letting me give up. She is my rock. I Love you!

ACKNOWLEDGMENTS

I would like to express my deepest gratitude to my advisors Dr. Ryan G. Toomey and Dr. Nathan D. Gallant for their constant support, guidance and encouragement throughout the duration of my PhD. Thank you for always being there for me not only for your support in the academic part of this journey but also for your moral support, understanding, and kind words of encouragement when I needed a boost. To my committee members Dr. John M. Wiencek, Dr. Mark Jaroszeski, and Dr. Garrett Matthews, for your guidance and contributions to my research.

I like to thank all the members from the Smart Materials Lab and Cellular Mechanotransduction and Biomaterials Lab for their help, guidance, friendship, for listening, and all the fun times that we spent in the lab as well outside the academic environment. In particular I would like to thank Kranthi Kumar Elineni for taking the time to serve as a mentor and pass on some of his knowledge and valuable skills that helped me progress in my research. I also want to thank him for his constant feedback, encouragement, friendship, and laughs.

Lastly I would like to thank my family for their unconditional love and for being my biggest cheerleaders. They have always been there for me lifting me up and giving me the strength to keep pushing myself.

Thank you everybody for being a great support group. I will always be grateful!

TABLE OF CONTENTS

LIST OF TABLES iv

LIST OF FIGURES v

ABSTRACT vi

CHAPTER 1: INTRODUCTION 1
- 1.1 Motivation and Significance 2
- 1.2 Objectives and Hypothesis 4
  - 1.2.1 Objective 1 4
  - 1.2.2 Objective 2 4
  - 1.2.3 Objective 3 5
- 1.3 Summary of Chapters 5

CHAPTER 2: BACKGROUND 8
- 2.1 Biomaterials 8
  - 2.1.1 Biomaterials Overview 8
  - 2.1.2 Biomaterials in Tissue Engineering 9
- 2.2 Cell Adhesion 10
- 2.3 Cells-Material Adhesion Interactions 11
- 2.4 Topography 13
- 2.5 Surface Chemistry 15
- 2.6 Influence of Surface Chemistry on Cell Response 15

CHAPTER 3: EXPERIMENTAL MATERIALS AND METHODS 18
- 3.1 PNIPAAm Synthesis 18
- 3.2 PNIPAAm Solution Preparation 19
- 3.3 Electrospinning 20
  - 3.3.1 Theory of Electrospinning 20
  - 3.3.2 Experimental Protocol 23
- 3.4 Spin Coating 24
  - 3.4.1 Spin Coating Principles 24
  - 3.4.2 Experimental Protocol 25
  - 3.4.3 Surface Preparation (Deposition Techniques) 26
    - 3.4.3.1 APTES 26
    - 3.4.3.2 PEGSAM 26

CHAPTER 4: FABRICATION AND CHARACTERIZATION OF PLATFORMS 28
- 4.1 Introduction 28

4.2 Materials and Methods 29
4.2.1 Substrate Preparation 29
4.2.2 Electrospinning Setup and Parameters 30
4.2.3 Imaging and Analysis 31
4.2.4 Statistical Analysis 31
4.3 Results and Discussion 31
4.3.1 Variation of Projected Fiber Density by Electrospinning 31
4.4 Conclusions 36

CHAPTER 5: CELL ADHESION AND CELL SPREADING ON NON-ADHESIVE SURFACES 38
5.1 Introduction 38
5.2 Materials and Methods 41
5.2.1 Cell Culture and Reagents 41
5.2.2 Imaging and Analysis 41
5.2.3 Statistical Analysis 42
5.3 Results 42
5.3.1 Topographic Enhancement of Cell Adhesion to PNIPAAm 42
5.3.2 Cell Adhesion on PNIPAAm, APTES and PEGSAM Surfaces with Varied Fiber Densities 44
5.3.2.1 PNIPAAm 44
5.3.2.2 APTES 45
5.3.2.3 PEGSAM 45
5.3.2.4 Comparison of PNIPAAm, PEGSAM and APTES for Each Fiber Density 45
5.3.3 Cell Spreading on PNIPAAm, APTES and PEG Surfaces with Varied Fiber Densities 50
5.3.3.1 PNIPAAm 50
5.3.3.2 APTES 50
5.3.3.3 PEG 51
5.3.3.4 Comparison of PNIPAAm, PEG and APTES for Each Fiber Density 51
5.4 Discussion 52
5.5 Conclusions 55

CHAPTER 6: CELL ADHESION AND SPREADING RESPONSE ON PHOTO-CROSSLINKED PNIPAAm THIN FILM COATINGS 57
6.1 Introduction 57
6.2 Materials and Methods 59
6.2.1 Substrate Preparation 59
6.2.2 Cell Culture and Reagents 59
6.2.3 Imaging and Analysis 60
6.2.4 Statistical Analysis 60
6.3 Results 61
6.3.1 Topographic Enhancement of Cell Adhesion to PNIPAAm Thin Films 61

6.3.1.1 Polystyrene Petri Dish Film Supports 61
6.3.1.2 Glass Cover Slip Film Supports 62
6.3.1.3 Comparison of Petri Dish with Glass Cover Slip Underlying Film Supports 62
6.4 Discussion 65
6.5 Conclusions 65

CHAPTER 7: CONCLUSIONS AND FUTURE WORK 67
7.1 Conclusions 67
7.2 Future Directions 69

REFERENCES 71

LIST OF TABLES

Table 1: Spaces between fibers 33

Table 2: PNIPAAm thickness (nm) 63

LIST OF FIGURES

Figure 1: Interactions of cells with the surface of a material 12

Figure 2: Schematic of PNIPAAm synthesis 19

Figure 3: Schematic of electrospinning setup 22

Figure 4: Taylor cone 22

Figure 5: Spin coater 25

Figure 6: Platform fabrication approach 29

Figure 7: Projected fiber density as a function of electrospinning time 32

Figure 8: Fiber mat morphology and density varied with electrospinning time 34

Figure 9: Average fiber diameter as a function of projected fiber density 36

Figure 10: Non-adhesive surface with non-adhesive surface topography 40

Figure 11: Cell adhesion on (A) glass, (B) PNIPAAm film and (C) PNIPAAm film covered with electrospun PNIPAAm Fibers (~30% fiber density) substrates 43

Figure 12: Fluorescence images of attached cells for all the underlying surface chemistries and fiber densities 47

Figure 13: (A) Cell adhesion on low (<15%), medium (15-60%) and high PNIPAAm fiber density (>60%) with PNIPAAm, APTES and PEGSAM underlying surface chemistry 48

Figure 14: (A) Cell spreading on low (<15%), medium (15-60%) and high PNIPAAm fiber density (>60%) with PNIPAAm, APTES and PEGSAM underlying surface chemistry 49

Figure 15: Cell adhesion on PNIPAAm films 63

Figure 16: Fluorescence images of attached cells on PNIPAAm thin films with petri dish and glass cover slip underlying film supports 64

ABSTRACT

The overall thrust of this dissertation is to gain a fundamental understanding of the synergistic effects between surface topography and chemical functionality of poorly adhesive materials on enhancing the adhesion of mouse embryonic fibroblasts. Cellular response to surface topography and chemical functionality have been extensively studied on their own providing valuable information that helps in the design of new and improved biomaterials for tissue engineering applications. However, there is a lack of understanding of the synergistic effect of microscale and nanoscale topography with chemical functionality and the relative impact and contribution of each in modulating cellular behavior. By understanding the relationship between these cues, in particular using materials that are poorly adhesive, this study will provide new clues as to how cells adapt to their environment and also suggest new dimensions of biomaterial design for fine-tuning cellular control.

A microstructure that combined non adhesive materials with defined surface topography and surface chemistry is presented, to assess and correlate the enhancement of mouse embryonic fibroblasts cell adhesion and spreading. Poly (N-isopropylacrylamide) or PNIPAAm electrospun fibers were overlaid on PNIPAAm thin films (100 nm) at various time points to investigate the role of topography on such coatings by keeping the chemical functionality the same. After doing this, several topographical patterns were developed, spanning from sparse to dense fiber mats, and

cell adhesion strongly depended on the relative available areas for attachment on either the fibers or the supporting surface. To gain a better understanding of this finding, two surface chemistries, non-adhesive (self-assembled monolayer of polyethylene glycol (PEGSAM) alkanethiol on gold) or an adhesive coating (3-aminopropyltriethoxysilane (APTES) on glass) with well characterized adhesive properties were included in this study to assess the effect of topographical cues provided by the PNIPAAm electrospun fibers on cellular responses. With the deposition of the PNIPAAm fibers onto a PEGSAM surface, cell adhesion increased to almost 100%, and unlike the PNIPAAm surface, cell spreading was significantly enhanced. With the deposition of PNIPAAm fibers onto APTES, both cell adhesion and spreading were unaffected up to 60% fiber coverage. For both surfaces, PNIPAAm fiber densities above 60% coverage lead to adhesion and spreading independent of the underlying surface. These findings indicate the presence of a sparse topographical feature can stimulate cell adhesion on a typically non-adhesive material, and that a chemical dissimilarity between the topographic features and the background enhances this effect through greater cell-surface interaction.

In addition to the aforementioned studies, cell response was also assessed on PNIPAAm thin films coatings with thicknesses ranging from 100 nm to 7 nm. Cell adhesion and spreading was enhanced as the thickness of the thin film decreased. This change was more noticeable below 30 nm, wherein 7 nm shows the highest cell adhesion and spreading enhancement. The results reported are preliminary results and further experiments will be conducted, to support the data. It is believed that cellular response was enhanced due to a change in surface topography at the nanoscale level.

CHAPTER 1: INTRODUCTION

This dissertation contains the study of the multiscale effects of topography and surface chemistry on cell adhesion to non-adhesive materials. Cell adhesion to extracellular matrix (ECM) is essential for cellular organization, survival and regulation of various functions: including cell spreading, migration and proliferation. It also plays an important role in tissue function, repair and regeneration [1]. Cells, when adhered to the extracellular matrix (ECM), can sense and respond to a variety of physicochemical properties of the surface that they come in contact with. The physicochemical properties of the surface include the local density and molecular nature of adhesive ligands; in addition to the surface chemistry, topography and stiffness. The nature of the adsorption of cell adhesion-mediating ECM molecules to the surface for integrin receptors recognition is significantly influenced by the physicochemical properties of the surface layer material [2]. It is important to indicate that when cells interact with the surface layer of a synthetic material; cells see a surface with an adsorbed layer of water and proteins from biological fluids, instead of a bare surface.

In the case that cells are not able to synthesize and deposit their own ECM due to not having the suitable or appropriate physicochemical environment they may undergo apoptosis giving rise to some pathological conditions with lethal consequences in some cases [3]. It is important to gain an understanding of the physical and chemical properties effects of a material on cell adhesion, to appropriately control cell-material

interactions to prevent non desired events leading to the rejection of an implant by the body. Also, the understanding of the synergistic effects of the material properties helps in the design of new and improved materials to perform certain biological functions by substituting or repairing different tissues such as bone, cartilage or ligaments and tendons, and even by guiding bone repair when necessary [4].

1.1 Motivation and Significance

The physical properties of the surface of a poorly adhesive material, including topographical features (or structures) in the micron to the nano size range, can modulate cell adhesion. The adhesive properties of a poorly adhesive material such as, PNIPAAm have been reported under different conditions and deposition techniques, but several conflicting findings have been reported. It has not been reported as to how the structure of the coating layer of PNIPAAm modulates cell adhesion. Protein adsorption on PNIPAAm surface occurs and yet this material is non- adhesive but in some cases has been shown to be adhesive.

PNIPAAm is a thermoresponsive polymer that undergoes a volume phase transition at a lower critical solution temperature of 32ºC in aqueous solutions. The polymer undergoes a volume phase change when increasing the temperature above its LCST, going from a single phase with swollen hydrophilic state to a collapsed hydrophobic state. The collapsed chains apparently adsorb protein, whereas the water-swollen state below the LCST is assumed to repel protein. However, several groups have shown dependence in PNIPAAm thickness, attributing it to a change in hydrophobicity and the method of preparation. Usually the change in hydrophobicity is

small. For example, PNIPAAm spin coated on a preconditioned silicon wafer did not adsorb human serum albumin either above or below the LCST, however it was observed on PNIPAAm hydrogels polymerized by electron beam irradiation on tissue culture polystyrene or on glass, that fibronectin adsorbed on thin (15-20 nm) PNIPAAm gels but not on thick (>30 nm) coatings [5-8]. Cells did not adhere on thicker gels repelling cells above and below the LCST, even though there was a 10º increase in the water contact angle on the dry, thick gels above the LCST [6, 8]. Plasma-deposited PNIPAAM coatings reversibly adsorb protein above 32ºC, regardless of the film thickness [8-10]. One group looked at the protein resistance of PNIPAAm brushes grafted from silicon wafers as a function of the chain molecular weight, grafting density, and temperature. Above LCST, very low levels of protein adsorb on densely grafted brushes, and the amounts of adsorbed protein increase with decreasing brush-grafting-densities. However, another group showed that protein adsorption on thick films (brushes) increased when compared to thin films [11].

Even though these findings are conflicting, it seems that there is a structure or thickness adhesion dependence that modulates PNIPAAm adhesive properties. This work was motivated by this premise. In this work we wanted to explore if topographic features in the form of overlaid micron scale fiber mats on PNIPAAM thin films (100 nm) or nanoscale textures supporting thin films (with various thickness) modulate PNIPAAm adhesive properties by assessing cell adhesion and spreading. In both cases, we can assess whether a topographical structure that was either introduced by the overlaid fiber mats or perhaps it was already present on PNIPAAm thin films when the film thickness is varied, can alter PNIPAAm adhesive properties while keeping the chemistry of the

surface the same. To help support this study, two well-studied surface chemistries with adhesive and non-adhesive properties are incorporated to help elucidate the role of surface topography in altering the material adhesive properties.

A fundamental understanding of the relationship of topographical and surface chemistry cues, when poorly adhesive materials are used, will provide valuable information as to how a biomaterial surface chemistry and topography can be tuned to control and achieve a desired cellular response.

1.2 Objectives and Hypothesis

The overall objective of this research is to gain an insight on how micro and nano environmental cues such as topography and surface chemistry modulate key cellular responses during initial interactions, including cell attachment, and spreading.

1.2.1 Objective 1

Our first objective is to develop a platform of fiber- based topographical surfaces that enable independent variation of surface chemistry and topography. The working hypothesis is that a stable structure with combined surface topography and surface chemistry it is suitable for mouse embryonic fibroblasts cell adhesion and spreading. To test this, electrospinning parameters as well as PNIPAAm solution conditions are optimized to allow the successful formation of fibers.

1.2.2 Objective 2

Our second objective is to investigate cell adhesion and spreading as functions of underlying surface chemistry and topography of poorly adhesive materials. The

working hypothesis is that cell adhesion, and spreading is influenced and enhanced by the interplay of topographical features of a fiber based network and its underlying surface chemistry, even though the materials have poor adhesive properties. To test the hypothesis that topography can enhance cell adhesion on non-adhesive surfaces, we employed surfaces with well-defined chemistries and varied the surface coverage with electrospun PNIPAAm fiber mats.

1.2.3 Objective 3

Our third objective is to investigate cell adhesion and spreading on PNIPAAm thin films with thicknesses ranging from 100 nm to 7 nm. The working hypothesis is that cell adhesion and spreading is enhanced below 30 nm due to the presence of nanoscale topography. To test the hypothesis PNIPAAm thin film coatings were spuncast on two types of substrates with distinctive surface rougness. By controlling the concentration of PNIPAAm in solution, PNIPAAm thin films with various thicknesses were created.

1.3 Summary of Chapters

Chapters 1 and 2 provide an overview of the motivation, significance, goal and objectives to conduct this research study as well as some background to the topics that are relevant to this subject.

Chapter 3 lists and describes the experimental methods and materials used to execute the research objectives.

Chapter 4 reports the electrospinning setup parameters and PNIPAAm solution properties used to create the microscale topography as well as the procedure for the surface chemistry deposition of PNIPAAm thin film, APTES and PEGSAM. In this chapter we also report results including the variation of projected fiber density by electrospinning showing an exponential rise with respect to collection time; the explanation as to why the data was separated into low, medium and high projected fiber density bins with respect to the fraction of spaces between fibers, and the average fiber diameter for each fiber density.

Chapter 5 presents results of the initial observation that fiber-based topographical features enhanced cell adhesion to PNIPAAm which motivated the study of the interplay between surface topography and surface chemistry on cell-material adhesion properties. Cell adhesion and spreading results on PNIPAAm, APTES and PEGSAM surfaces with low, medium and high projected fiber densities are presented. These results revealed that cell adhesion was enhanced in the presence of poorly adhesive surfaces before decreasing to approximately 50% attachment on the highest fiber density. Cell spreading area was influenced differently with respect to each projected fiber density and surface chemistries groups. Adherent cell spreading area on PEGSAM was enhanced before decreasing on the highest fiber density. A similar trend was observed for APTES. Cell spreading was minimal on PNIPAAm and unchanged by fiber density.

Chapter 6 reports preliminary results of cell adhesion on PNIPAAm thin films spuncast on two type of substrates; petri dish and glass covered slip. Preliminary results suggest that cell adhesion was enhanced on both types of substrates as the thickness

of the film got thinner, due to the presence of nanoscale topography rather than just a thickness reduction effect.

Finally, Chapter 7 presents overall research conclusions and provides directions for future studies in an attempt to complete the experiments necessary to complete studies from Chapter 6.

CHAPTER 2: BACKGROUND

2.1 Biomaterials

2.1.1 Biomaterials Overview

A biomaterial is referred to as “any material, natural or man-made, that comprises whole or part of a living structure or biomedical device which performs, augments, or replaces a natural function” [12]. The surface characteristics of a biomaterial both chemically and physically, determine the interaction between the living host tissue with the implant [13, 14]. These material properties remain throughout the lifetime of the implant. The physical and chemical properties of the biomaterial can be modified to mimic the properties of tissues which they are meant to enhance or substitute [15, 16]. An understanding of the interactions of cells with materials helps in the development of new materials for biological applications.

Advancements in the field of biomaterials and tissue engineering have represented the development of biomaterials, with well-defined templates that emulate native properties of the extracellular matrix (ECM). Throughout the years, the design of biomaterials has evolved, allowing the use of more materials, as well as the integration and control over the surface properties desired for a specific application.

There are two main strategies for modulating cell–material interactions. The first strategy involves the construction of an inert surface that resists protein adsorption to

ensure that cell adhesion does not occur [17]. If cell adhesion does not occur, no activation of the immune system, blood coagulation, thrombosis, extracellular matrix deposition and other interactions between material and surrounding environments takes place. This type of biomaterial has been used to fabricate implants in which protein adsorption is not desired such as, parts of joint prostheses [18], and blood-contacting medical devices [18, 19]. The other strategy to modulate cell–material interactions is to construct biomaterials that support cell–material interactions in a well-regulated manner. These interactions will likely promote protein adsorption to the biomaterial surface leading to cellular response such as: cell adhesion, migration, proliferation, differentiation, long-term viability and cell functioning (contraction or secretion of extracellular matrix) [17].

The design of these two types of surfaces requires special attention to the physical and chemical properties of the material to lead to the optimal control over the desired interaction between the cell and its surroundings.

2.1.2 Biomaterials in Tissue Engineering

One of the primary uses of biomaterials is to replace hard or soft tissue that has been damaged or destroyed [20]. Tissues and organs in the body may experience some type of destructive process such as: fracture, infection, deformity, failure, and loss of function or damage by a disease. The tissue and structures that have been damaged may be removed and replaced with a synthetic biomaterial [21]. Physicians primarily treat organ failure or tissue loss by performing organ transplantation; from a donor to a recipient or from the patient's own tissue from one site to another; or reconstructive

surgery [22]. Even though these surgical procedures have benefited a lot of lives, they have their challenges. The need of organ donors is much higher compared to the number of people that are organ donors [23].

Every day in the United States 18 people die waiting for an organ and more than 117,000 men, women, and children await life-saving organ transplants [23, 24]. Another challenge with organ transplants is the rejection of the transplanted organ by the body due to the reaction of the antibodies in the blood stream to the new organ resulting in organ failure.

2.2 Cell Adhesion

Mammalian cells have the fundamental property of adhering to surfaces or to other cells. The cell adhesion process can be divided into major phases; including cell attachment, cell spreading, actin filaments assembly and the formation of focal adhesion complexes. This process is mediated by transmembrane proteins known as cell adhesion molecules (CAMs). These proteins can be classified into four groups, which include integrins, cadherins, selectins, and the Immunoglobulin superfamily [25]. These transmembrane adhesion proteins link the cytoskeleton to extracellular ligands. Cell to cell adhesion is usually mediated by cadherins. Cadherins play an important role in cell adhesion because they form adherens junctions to bind cells together to form tissues[26].

Cell adhesion to the ECM is primarily mediated by the integrin family of receptors [27]. Integrins are heterodimers that bind to specific sites on ligands such as fibronectin, collagen and laminin. Integrins couple the ECM outside a cell to the cytoskeleton inside

the cell. They function as transmembrane linkers allowing the cell to grip the matrix and apply tension via the cytoskeleton contractility. Integrin mediated adhesion begins with a conformational change in the receptor resulting in mechanical coupling to the ligand [28]. It is then followed by the clustering of bound receptors to form focal adhesions, supramolecular complexes that strengthen adhesion and transmit signals [29]. Cell adhesion to the ECM is a well regulated and critical process because it can direct proper cellular response and determine cell fate.

2.3 Cell-Material Adhesion Interactions

The adhesion interactions that take place between cells and synthetic materials are primarily mediated by the proteins adsorbed from biological fluids onto the surface layer of the material [2]. Cells never see a bare surface; they see a surface that has been previously coated with water and proteins. As soon as a material has been implanted the protein adsorption takes place and cells recognize this foreign surface through the adsorbed layer [3]. Initially cells respond to the adsorbed proteins, rather to the surface itself [2, 30]. (See Figure 1).

When cells are incubated on a material substrate or come in contact with an implant in the body, the proteins from culture media or from the biological fluid adsorb on the material surface layer. When a cell encounters the adsorbed protein, integrin receptors bind, bound receptors cluster, the cytoskeleton is reorganized and the cell actively spreads onto the material surface. Mechanical forces are generated by the contraction of the actomyosin cytoskeleton spanning between adhesion sites. The cytoskeleton of all anchorage dependent cells is maintained in a state of mechanical

tension generated by myosin motors and transmitted by the actin fibers. This mechanical tension is balanced by microtubules, which are involved in maintaining the structure of the cell, but mostly by cell-ECM adhesion or cell-cell adhesion. Microtubules together with microfilaments and intermediate filaments form the cytoskeleton. Lastly, cells synthesize ECM proteins at interface between the cell and the substrate [31].

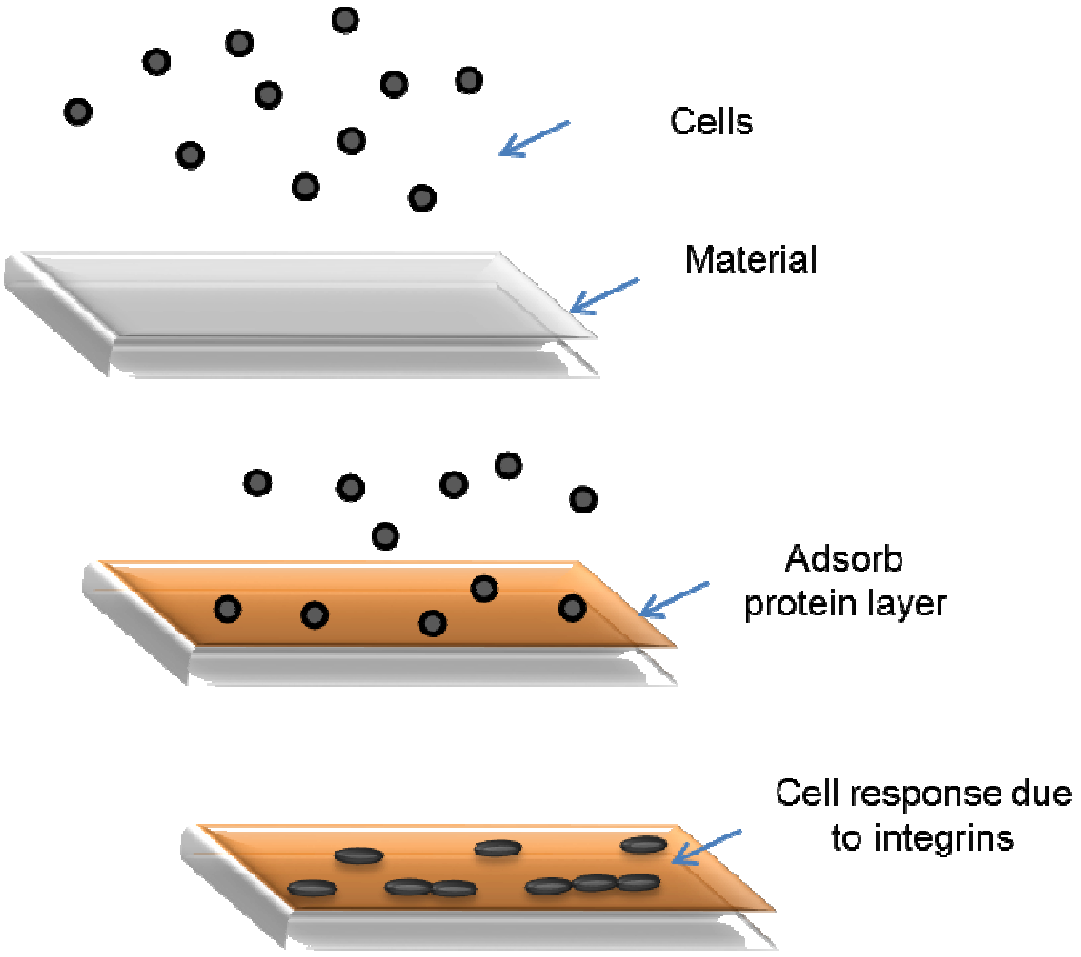

Figure 1: Interactions of cells with the surface of a material

2.4 Topography

It has been of knowledge for years that cells interact and react to the topography of the environment they are attached to [31]. The influence of surface topographic structures on cell response has been extensively studied since then, providing valuable information about the control exerted over shape, orientation and adhesion of cells [32]. Throughout the years the advance in micro-technology has allowed the fabrication of more accurate and diverse microscale and nanoscale topographical features, and the use of a wide range of biocompatible materials. Methods such as photolithography (PL), electro-beam lithography, microcontact printing, and electrospinning have been reported for the fabrication of these substrates and allowing for the engineering of its properties and patterning of a wide range of biomaterials [33].

When a biomaterial is fabricated, whether it is for in vitro studies, a prosthetic device or an implant, it is likely that some type of topography will be created intentionally or by accident [34]. In the case that the topography is created by accident, it might not be noticeable at the macroscale level. When topography has been created intentionally on the surface of a material, the scale and the type of topography dictates the effects that topography has on cellular response [35, 36].

In 1911, Harrison studied the interactions of cells grown on spider web fibers with the fibers surface topography [37]. Another early work in topography, specifically with contact guidance on fibers and grooves showed that cells aligned and migrated along these features [38]. It was shown that cells most likely reacted to the properties of the features, such as curvature and not to the molecular orientation of the substrate.

Surfaces with well-defined features, including islands, pillars, grooves and ridges, have been used for cell response to topography studies [39]. Cellular response has been compared for a smooth surface with a groove like pattern surface while keeping the chemistry of the surface the same. It was observed that cells on the grooves were elongated and oriented along the grooves and cell height was ~1.5-fold greater than that of cells on the smooth surface. Fibroblasts have exhibited a similar elongated structure, and branched shapes on substrates with less actin stress fibers compared to smooth surfaces [40]. In this same study, migration was assessed showing that, the transmigration between micropillars depends on the spacing between the micropillars.

The effect of contact guidance has been also observed when fibers within an electrospun scaffold are aligned. Leong et al. observed that aligned electrospun fibers enhanced human Schwann cells maturation more than randomly oriented fibers [41]. Schwann cells aligned and elongated unidirectionally along the fiber axis when cultured on aligned fibers. When cultured on random fibers, they were randomly oriented. Aspects of the fibrous scaffolds such as pore size, porosity and fiber diameter have been shown to affect cell response [42]. Scaffold design can be tailored to control cell migration through the scaffold.

Surface roughness can also influence cell behavior by modulating cell morphology, proliferation and phenotype expression. It has been reported that cells that are in contact with microrough surfaces, are stimulated towards differentiation in comparison with cells on smooth surfaces. One example of this behavior is that implants with microtextured titanium surfaces enhance bone formation in vivo and osteoblast phenotypic expression in vitro. It has been observed that cells cultured on Ti

surfaces with microrough features exhibit reduced proliferation but differentiation is enhanced when compared to cells grown on tissue culture plastic or smooth Ti substrates [43].

2.5 Surface Chemistry

Protein adsorption to the surface plays an important role in cell adhesion, since it mediates cell adhesion and also provides signals to the cell through the cell adhesion receptors. The activity of protein-coated substrates can show a dependence on the choice of substrate and its characteristics. Adsorbed proteins including immunoglobins, vitronectin, fibrinogen, and Fibronectin (FN) mediate the attachment of cells to the substrate. It has been shown that hydrophobic surfaces tend to absorb more proteins, while hydrophilic surfaces tend to resist protein adsorption [44].

2.6 Influence of Surface Chemistry on Cell Response

The surface chemistry of biomaterials can modulate in vitro and in vivo cellular responses including adhesion, survival, cell cycle progression, and expression of differentiated phenotypes [45, 46]. Difference in cellular responses to biomaterial surface properties can be attributed to the difference in adsorbed proteins species, concentration and/or biological activity [47]. Cell-material interactions are mediated by the proteins adsorbed onto the surface of the material and provide signals to the cell through the cell adhesion receptors [48]. The adsorption of the proteins occurs right after the biomaterial is implanted into the organism or comes into contact with cell culture environment. These cell-material interactions regulate cell and host responses to implanted devices, biological integration of biomaterials and tissue-engineered

constructs, and the performance of cell arrays and biotechnological cell culture supports [45, 46]. The design of biomaterials requires an understanding on how a material property such as surface chemistry affects cellular behavior, to be able to incorporate or modify biologically relevant properties into the biomaterial. Material surface properties can consist of the hydrophobicity, charge, roughness, elasticity, and chemical composition of the material.

The surface hydrophobicity can govern cell response and it is measured by contact angle. The lower the contact angle the more hydrophilic the surface is. Some studies have shown that the more hydrophilic the film is, the higher the cell adhesion is to the surface [44, 49, 50]. It has been shown that fibroblasts have maximum adhesion when contact angles are between 60º to 80º [51]. In the case of osteoblasts, adhesion has been reported to decrease as the contact angle on the surface is increased from 0º to 106º. Anionic and neutral hydrophilic surfaces increase macrophage monocyte apoptosis and reduce macrophage fusion to modulate inflammatory responses to implanted materials [52].

Protein adsorption to the surface plays an important role in cell adhesion, since it mediates cell adhesion and also provides signals to the cell through the cell adhesion receptors. The activity of protein-coated substrates can show a dependence on the choice of substrate and its characteristics. Adsorbed proteins including immunoglobins, vitronectin, fibrinogen, and Fibronectin (FN) mediate the attachment of cells to the substrate. It has been shown that hydrophobic surfaces tend to absorb more proteins, while hydrophilic surfaces tend to resist protein adsorption [44]). García and coworkers, for example, cultured myoblast cells on two different types of polystyrene [53]. Although

both surfaces were coated with similar densities of fibronectin, cells proliferated on one substrate but differentiated on the other. The patterning of surface chemistry has shown to have an influence on cell motility, an effect similar to contact guidance [54].

CHAPTER 3: EXPERIMENTAL MATERIALS AND METHODS

3.1 PNIPAAm Synthesis

The monomer methacroylbenzophenone (MaBP) was synthesized following the protocol previously reported by our group [55]. The copolymer PNIPAAm was synthesized using N-Isopropylacrylamide (NIPAAm), 3 mol % of MaBP and 0.1mol% AIBN as the initiator via free-radical polymerization. Figure 2 shows both reactions. The reaction was carried out in dioxane for 18 hours at 65 ºC. The sample was degassed with nitrogen by freeze-thaw cycles prior to reaction. The polymer was precipitated in diethyl ether and dried under high vacuum. The structure was confirmed with NMR. All reagents were purchased from Sigma. Acetone and dioxane were distilled from calcium hydride before use, and NIPAAm was recrystallized from hexanes. All other reagents were used as received.

This copolymer is a photocrosslinkable thermoresponsive polymer that undergoes a reversible volume phase transition; going from a swollen hydrophilic state to a collapsed hydrophobic state when cued by changes in temperature. Since this copolymer has the characteristic of being photocrosslinkable it allows the fabrication of stable fiber based platforms by preventing them from disintegrating. It also offers the opportunity of building surfaces with different elastic modulus and uniformity. This copolymer was selected for these studies because it has shown low protein adsorption and cell adhesion when it is present in it is uniform state making it desirable for these

studies to show that in fact a topographical change can enhance cell attachment and spreading [56-58].

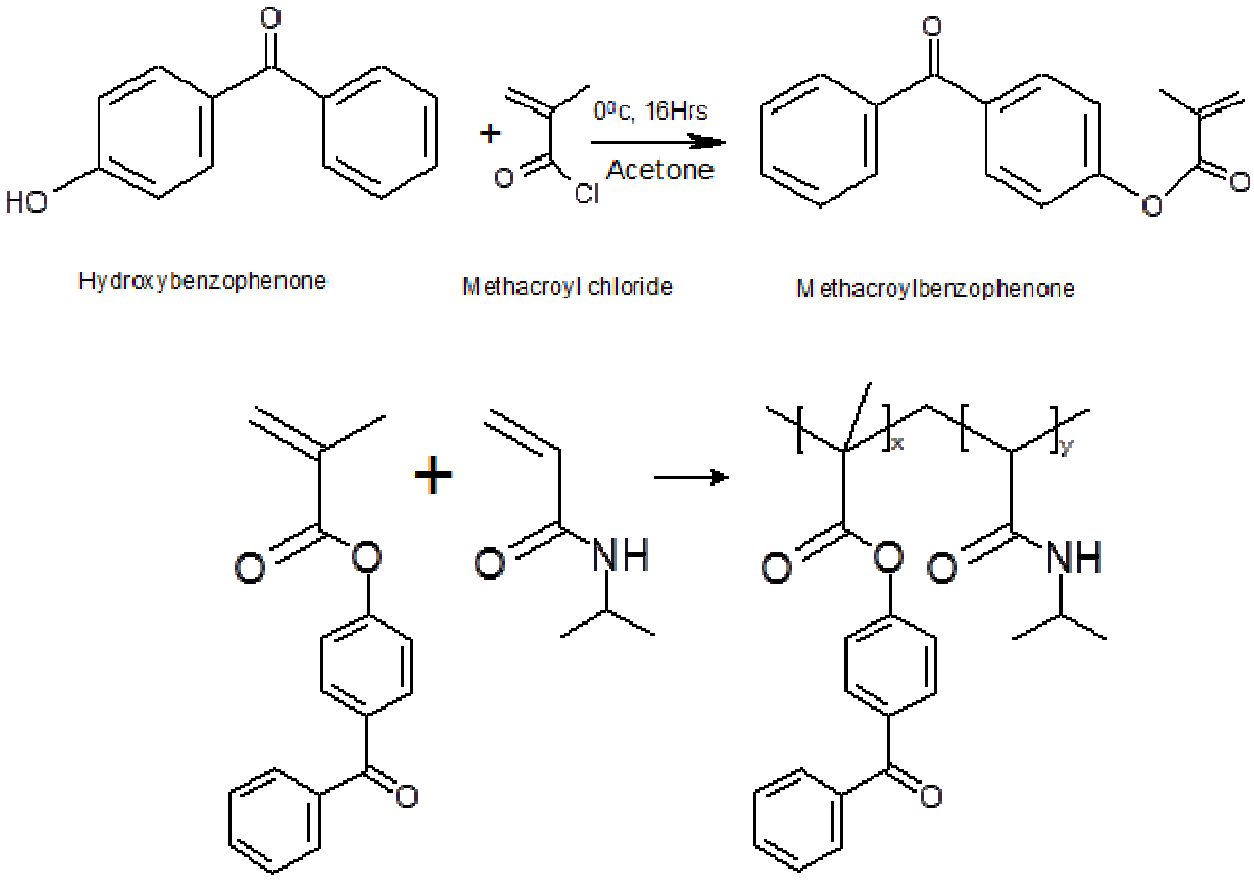

Figure 2: Schematic of PNIPAAm synthesis

3.2 PNIPAAm Solution Preparation

1. PNIPAAm Solution for Electrospinning

    a. A 15 wt % PNIPAAm solution in isopropanol was dissolved overnight.

    b. Filtered with a 0.45 μ filter prior to use.

2. PNIPAAm solution used for the preparation of 100 nm thin film

a. A 3 wt % PNIPAAm solution in cyclohexanone was dissolved overnight.

b. Filtered with a 0.45 μ filter prior to use.

3. PNIPAAm solution used for the preparation of thin films with different thicknesses

a. A series of PNIPAAm solutions in ethanol were prepared (3 wt %, 2 wt %, 1 wt %, 0.5 wt %, 0.25 wt %, 0.125 wt %) and dissolved overnight.

b. Filtered with a 0.45 μ filter prior to use.

3.3 Electrospinning

3.3.1 Theory of Electrospinning

Electrospinning is a technique that involves the use of high voltage on an electrically charged polymer solution or melts to draw out a jet between two electrodes, which dries creating a polymer fiber. The equipment necessary for this technique consists of four major components: a high voltage power supply, a syringe pump, a metal syringe needle, and a stationary grounded target to collect the produced fibers, (See Figure 3) [59].

In a typical electrospinning set-up, a polymer solution or melt is dispensed through a metal needle that is attached to a syringe [60]. The flow rate at which the solution is dispensed is controlled with a positive displacement syringe pump. High voltage is applied to the needle, which contains the polymer fluid held by its surface tension, inducing a charge on the surface of the liquid. The electrostatic repulsion causes a force directly opposite to the surface tension. As the intensity of the electric

field is increased, the pendant drop formed at the tip of the needle is elongated, forming a conical shape known as Taylor cone [61, 62]. At this point electrostatic repulsion and surface tension are balanced reaching an equilibrium point. When the electric field supplied surpasses a critical value, the electrostatic force within the charged solution overcomes its surface tension, and a charged jet is ejected from the Taylor cone accelerating towards the grounded target (Figure 4). As the jet travels, the charge moves to the surface of the fibers due to the evaporation of the solvent changing the current flow mode from ohmic to convective. Even though the jet ejected from the Taylor cone is stable flowing away in a nearly straight line, it becomes unstable entering a bending instability also referred to as whipping instability region, in which the jet is bent back and forth achieving a spiral path. This process is triggered by electrostatic repulsion initiated at small bends in the jet. During this process the diameter of the jet is being reduced causing thinning and stretching. As the jet travels, the remaining solvent evaporates, leaving a charged fiber. The fiber proceeds to the grounded collector, wherein fibers are randomly deposited in the form of a non-woven scaffold. Typically a flat electrode is used to collect the fibers that are being randomly deposited.

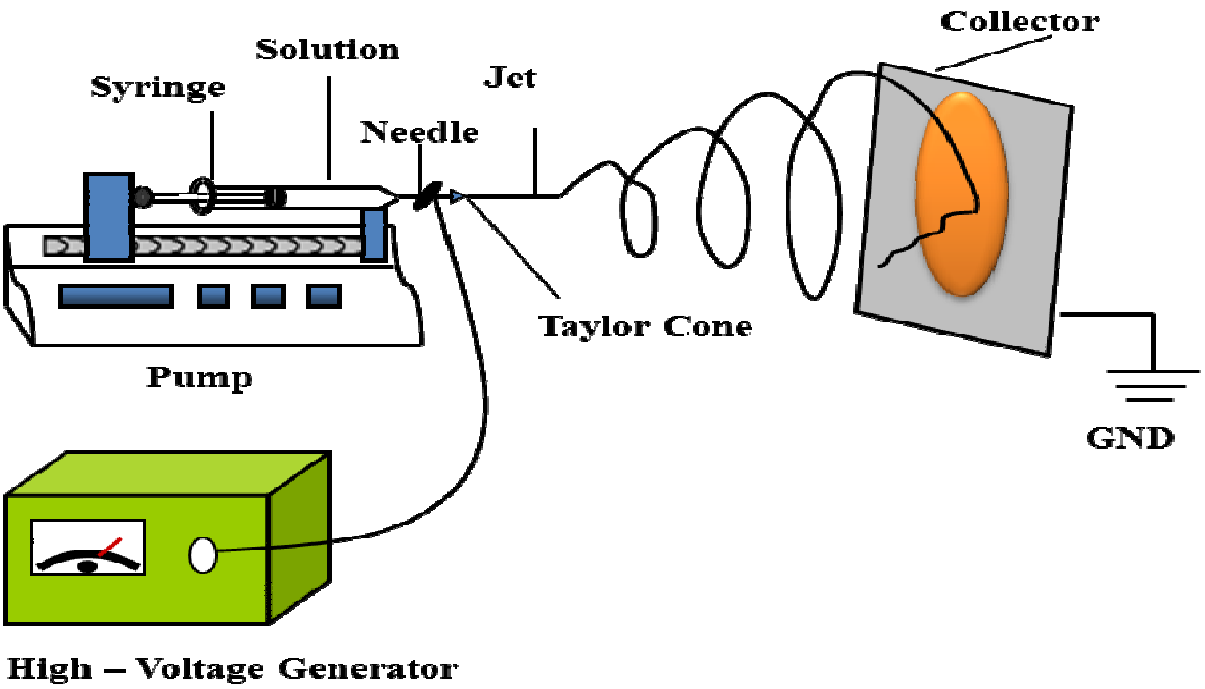

Figure 3: Schematic of electrospinning setup

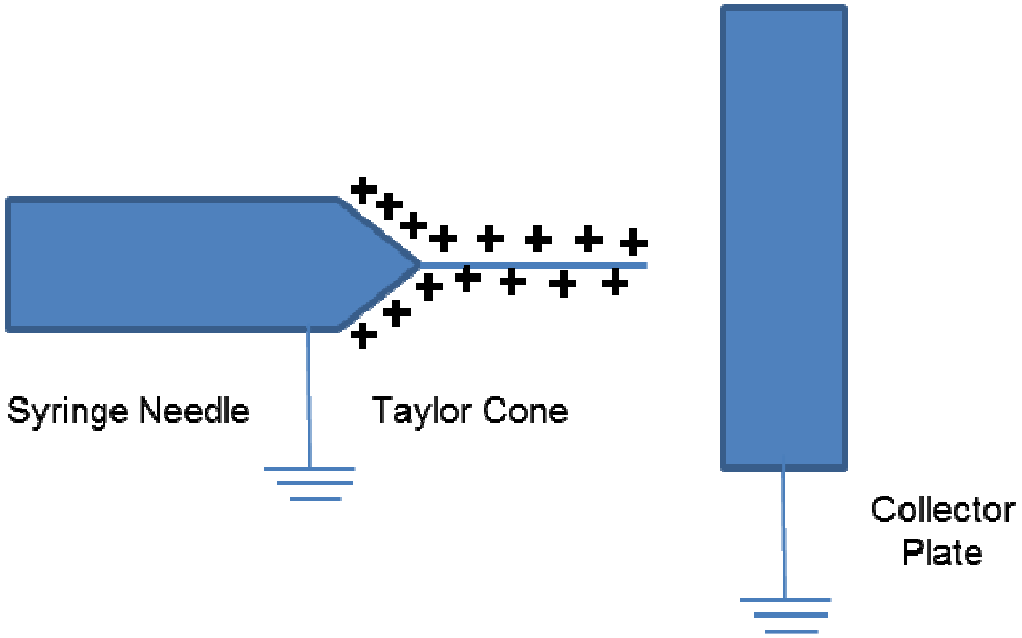

Figure 4: Taylor cone

3.3.2 Experimental Protocol

1. Electrospinning setup parameters were established

    a. Needle inside diameter - 22 gauge stainless steel blunt needle

    b. Needle size – 1 mL

    c. Flow rate - 1 mL/h

    d. Voltage - 15 kV

    e. Distance from needle location to conductive material at ground - 15 cm

    f. Conductive material at ground (0V)

2. Solution Properties

    A 15 wt % PNIPAAm solution in isopropanol was dissolved overnight.

3. Electrospinning procedure

    a. A 25 mm glass cover slip previously treated with the desired surface chemistry is glued onto the grounded target.

    b. The high voltage generator in turn on and once it reaches 15 kV the electrospinning deposition is timed. The times of deposition used were 10s, 30s, 50, 90s, and 300s.

    c. The substrate is removed from the grounded target and The PNIPAAm fiber mats were then cross-linked by UV light (365 nm) for 30 min.

d. Steps a through c are repeated for each surface chemistry, including PNIPAAm, APTES and PEGSAM.

3.4 Spin Coating

3.4.1 Spin Coating Principles

A spin coater is a common method used to apply a thin film of uniform thickness to flat substrates (Figure 5). It is often used in micro fabrication for the production of photoresists. In a typical spin coating process the first step consists of placing the substrate into the spin coater which is held in place by applying vacuum [63, 64]. The deposition of the thin film is usually done in three steps. The first step is the dispense step and it can be done two ways; in the static dispense the solution is dispensed to the center of the substrate surface, and in the dynamic dispense the solution is dispensed while the substrate is rotating at a slow speed allowing the solution to spread. It is then followed by a high speed step, to spread the fluid (in the case of the static dispense) and thin the fluid. The typical spin speeds range from 1500 – 6000 rpm which depends on the solution and substrate properties and it can take from 10 s to several minutes. The high speed and time generally defines the thickness of the film. In this step the solution flows radially due to the centrifugal force and the excess solution is ejected off the edge of the substrate. The film continues to thin slowly as it dries up to a point that disjoining pressure causes the film to reach an equilibrium thickness or until the viscosity increases due to the solvent evaporation. The last step consists of a drying step which is sometimes included to remove excess solvents from the film without

considerably thinning the film. This process is done under a fume hood because the coating material is usually volatile.

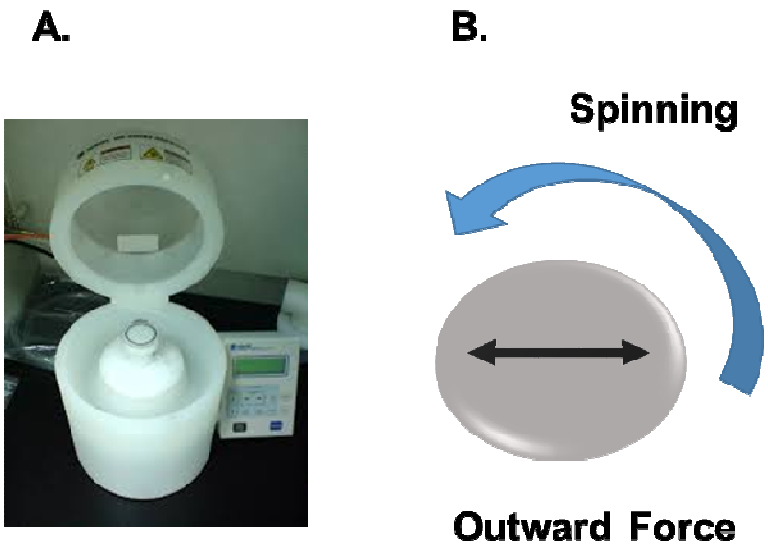

Figure 5: Spin coater

3.4.2 Experimental Protocol

1. PNIPAAm solution in cyclohexanone

PNIPAAm solution was dispensed on a 25 mm glass cover slip that was previously coated with APTES, by static dispense [65]. The solution was accelerated to a high speed of 2000 rpm for 45 s. The substrate was then removed and cross-linked by UV light (365 nm) for 30 min.

2. PNIPAAm in ethanol solution

PNIPAAm solution was dispensed on a 25 mm glass cover slip that was previously coated with APTES or polystyrene petri dish, by dynamic dispense at 150

rpm for 15 s [66]. The solution was then accelerated to a high speed of 6000 rpm for 30 s. The glass cover slip was attached to a silicon wafer to avoid deformation of the substrate due to the vacuum that holds the substrate in place, inducing the production of patterns on the surface of the substrate.

3.4.3 Surface Preparation (Deposition Techniques)

3.4.3.1 APTES

1. The substrate, a 25 mm round cover slip was first sonicated in ethanol for 15 min.

2. Blown dry with nitrogen.

3. Plasma cleaned for 5 min.

4. The substrate was placed in a glass container

5. A 1 v/v% solution of APTES in acetone was dispensed into the glass container

6. The substrate was soaked in the solution for 15 min.

7. Rinsed with acetone.

8. Dried in an oven for 10 min. at 110ºC.

3.4.3.2 PEGSAM

1. The substrate, a 25 mm round cover slip was first sonicated in ethanol for 15 min.

2. Blown dry with nitrogen.

3. Plasma cleaned for 5 min.

4. Thin films of titanium and gold (10 nm and 20 nm, respectively) were sequentially deposited on the substrate by electron-beam deposition.

5. The substrates were submerged in 2 mM triethylene glycol mono-11-mercaptoundecyl ether (Aldrich) in ethanol (200 proof) for 2 hours and blown dry with a stream of nitrogen gas.

CHAPTER 4: FABRICATION AND CHARACTERIZATION OF PLATFORMS

4.1 Introduction

Composite surfaces have been fabricated to study the combined effect of surface topography and chemical functionality in cellular response. The combined effect of these properties has shown that cells respond more to one property over the other, but the contribution of each property is not well understood. Due to the lack of understanding of the interplay between surface topography and chemical functionality in modulating cellular behavior, emerged the idea of studying how the adhesivity of a surface that typically does not support significant cell adhesion may be altered by the presence of topographical features, even if those features are poorly adhesive as well. The fabrication of a structure that combined surface topography and chemical functionality with materials that are typically non-adhesive to cells was needed in order to conduct this study.

The structure or platform fabrication approach is shown in Figure 6. The surface topography consists of PNIPAAm fibers, which is a poorly adhesive material, laid on a substrate at different time points creating different distinctive topographies In order to create the fibers, electrospinning was the method of preference due to the simple setup and easy way of creating fibers and extensive use in tissue engineering [67]. Prior to the deposition of the electrospun fibers the surface chemistry is incorporated to the substrate. Two of the chemistries have well-characterized, disparate adhesive

properties, APTES (adhesive coating) and PEGSAM (non-adhesive), and the third one is a smooth PNIPAAm thin film [68-70].

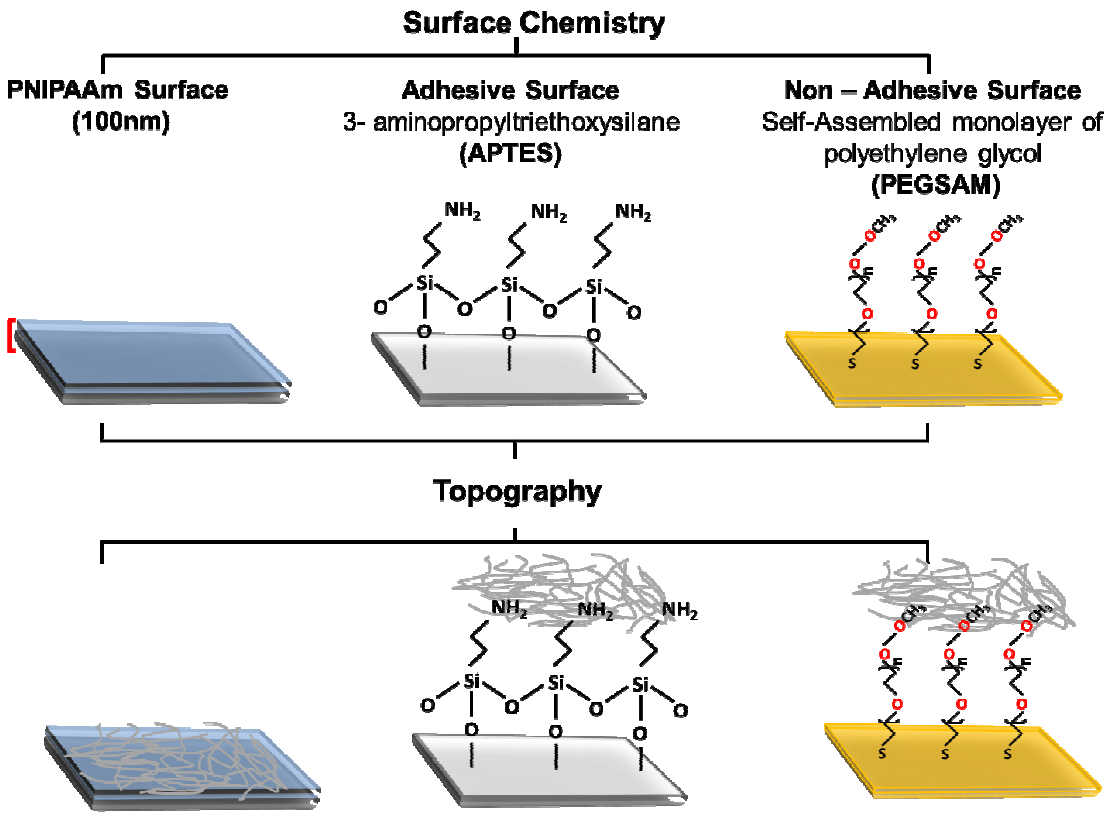

Figure 6: Platform fabrication approach

4.2 Materials and Methods

4.2.1 Substrate Preparation

The substrate used was a 25 mm round glass cover slip and it was treated either with APTES or PEGSAM. The APTES substrates were submerged in a solution of 1.0 v/v% 3-aminopropyltriethoxysilane for 15 minutes, rinsed with acetone and dried at 110ºC for 10 minutes [55, 68, 69]. For the preparation of the PEGSAM surfaces, the

glass cover slips were sonicated in ethanol for 15 minutes, blown dry with a stream of nitrogen gas and oxygen plasma cleaned [70]. Thin films of titanium and gold (10 nm and 20 nm, respectively) were sequentially deposited on the substrate by electron-beam deposition. The substrates were then submerged in 2 mM triethylene glycol mono-11-mercaptoundecyl ether (Aldrich) in ethanol (200 proof) for 2 hours and blown dry with a stream of nitrogen gas.

For the preparation of PNIPAAm thin films, the glass substrates were treated with APTES, following the protocol already described. A solution of PNIPAAm in cyclohexanone (3 wt %) was spuncast at 2000 rpm for 45s onto the APTES treated glass substrate. The substrate with the polymer film was cross-linked by UV light (365 nm) for 30 min. Film thickness was assessed by ellipsometry [65].

4.2.2 Electrospinning Setup and Parameters

The electrospinning set up consisted of a high voltage power supply (Gamma High Voltage), and variable syringe pump (KD Scientific). A concentration of 15 wt % of PNIPAAm was prepared in isopropanol (Sigma). The PNIPAAm solution was dispensed via a 22 gauge stainless steel blunt needle (Small Parts) attached to a 1mL syringe (Becton Dickinson) at a constant flow rate of 1 mL/h and a voltage of 15 kV was supplied. The distance between the tip of the needle and the grounded collecting plate was 15 cm. The fibers were collected on a 25 mm glass cover slip placed on the grounded collecting plate. For the preparation of platforms with different surface fiber density the time of electrospinning was controlled; thereby controlling the amount of fibers deposited onto the grounded plate. The times of deposition used were 10s, 30s,

50, 90s, and 300s. The PNIPAAm fiber mats were then cross-linked by UV light (365 nm) for 30 min.

4.2.3 Imaging and Analysis

Fiber density was extracted from phase contrast images. The projected surface fiber density was estimated by using an image analysis thresholding algorithm. The same binary mask was used to measure the size of each area not covered by fibers. Images (phase contrast, red and green fluorescence) at 10 locations were acquired for each sample and the data were reported as the mean ± SD of at least 3 experiments.

4.2.4 Statistical Analysis

Experiments were performed in triplicate in at least three independent experiments. Data are reported as mean ± SD, and statistical comparisons using SigmaPlot 11 (Systat Software, San Jose, CA) were based on analysis of variance and the Holm-Sidak test for pairwise comparisons, with a p-value < 0.05 considered significant.

4.3 Results and Discussion

4.3.1 Variation of Projected Fiber Density by Electrospinning

To understand the role of topography in enhancing cell adhesion despite the poor adhesivity of the material, we used collection time to vary the surface density of electrospun fibers upon PNIPAAm and well-defined adhesive and non-adhesive chemistries (PEGSAM and APTES, respectively). Prior to the deposition of electrospun fibers, the target substrates were coated with APTES, PEGSAM or a cross-linked

PNIPAAm film. Randomly oriented electrospun fibers were collected for 10s, 30s, 50s, 90, or 300s on batches of substrates placed on a grounded collecting plate (Figure 7). The projected fiber area coverage followed an exponential rise with respect to collection time [projected coverage = $a\left(1-e^{(-bt)}\right)$]. This was attributed to the decreasing probability of surface area coverage for each additional fiber; i.e. the first fiber has a 100% probability of directly covering the surface, the second fiber has a slightly lower probability due to fiber overlap, and so on.

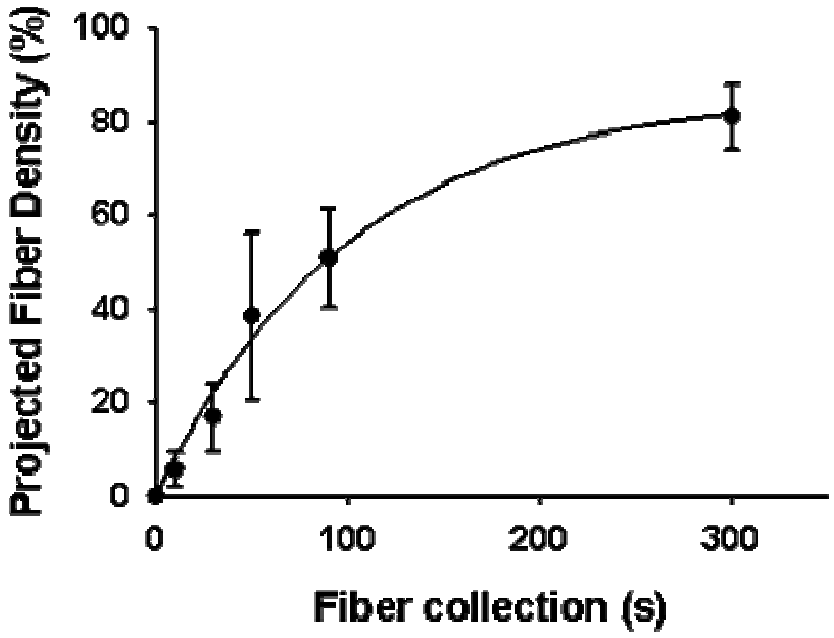

Figure 7: Projected fiber density as a function of electrospinning time. Fiber coverage exhibited exponential rise to saturation behavior with respect to time [projected coverage = $a\left(1-e^{(-bt)}\right)$].

Although we varied the projected surface fiber coverage with time of electrospinning on a global scale, local differences in fiber density were also present

due to the instability of the polymer jet during electrospinning. This instability generated random patterns of fibers independent of the underlying substrate (Figure 8). Therefore, in order to account for these slight variations, the data were separated into low, medium and high projected fiber density bins which corresponded to less than 15% global fiber coverage, 15% - 60% global coverage, and greater than 60% global coverage, respectively (Table 1).

Table 1: Spaces between fibers

	Mean area (μm^2)	S.D. area (μm^2)	Fraction >250 μm^2	Fraction >700 μm^2	Fraction >7000 μm^2
Low fiber density	1120	482	0.51	0.33	0.03
Medium fiber density	267	80	0.36	0.09	0.00
High fiber density	66	16	0.02	0.00	0.00

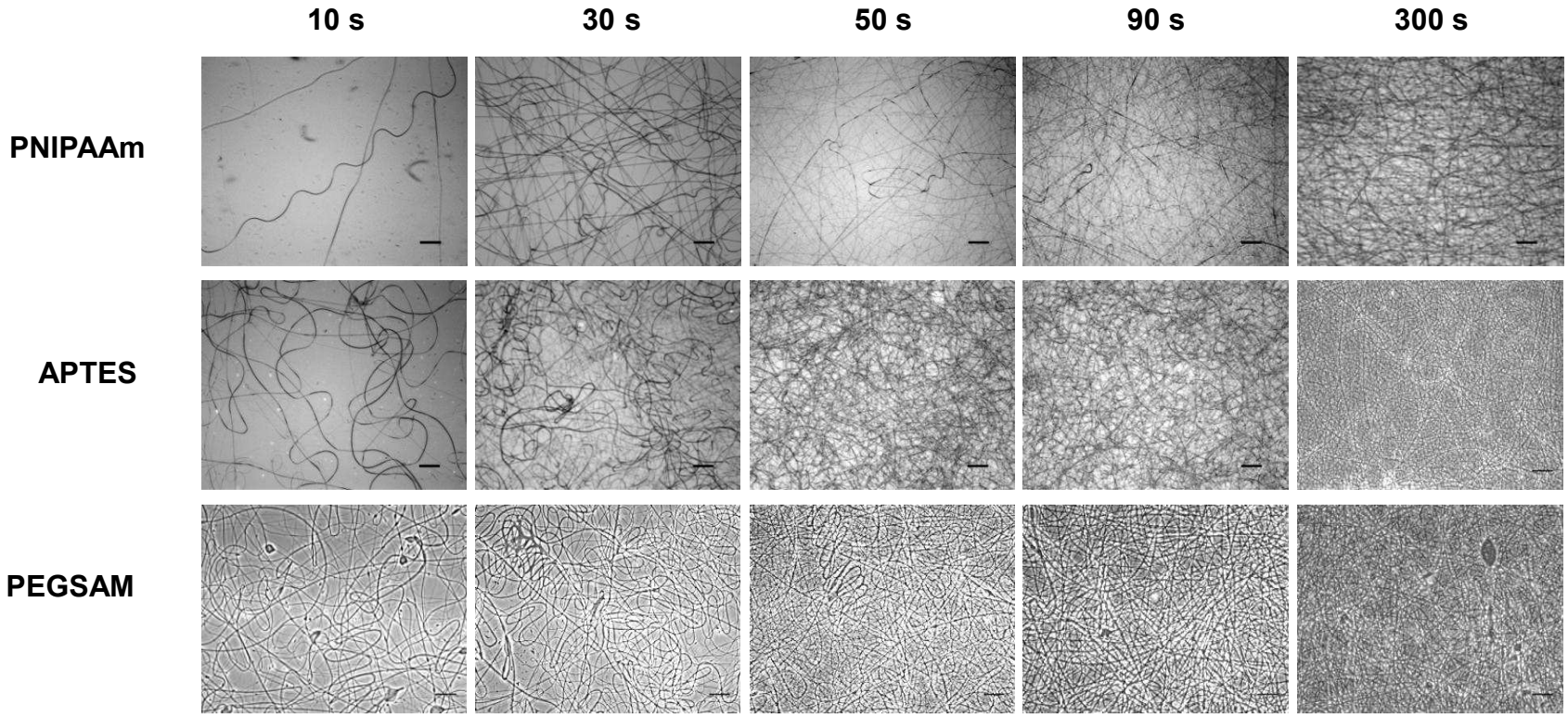

Figure 8: Fiber mat morphology and density varied with electrospinning time. The overlap of fibers resulted in contrasting surfaces: low fiber density (2D topography), medium fiber density (transition from 2D to 3D) and high fiber density (3D topography) with minimally exposed support surface. (bars = 100 μm)

These ranges were chosen so that at low fiber coverage (<15%), the average spacing between fibers was greater than the maximum cell size with 3% at least 10 times the area of a fully spread cell; at medium fiber coverage (15-60%), the average spacing between fibers was greater than minimally spread cells with 9% of spaces exceeding the maximum cell size; and at high fiber coverage (> 60%), the average spacing was less than the cell size. The fiber densities at low and medium coverage were utilized to study how two-dimensional spacing between physical features affects cell adhesion and spreading. Fiber coverage above 60% forms a prominent 3D mesh-like surface and was expected to prevent most cells from accessing the underlying substrate.

Well characterized surface chemistries were also employed to provide a better understanding on how topography and the underlying surface collectively regulate cell adhesion and spreading. Statistical fiber diameter distributions in the three projected fiber density bins were obtained in order to evaluate if the instability of the polymer solution jet, time of electrospinning, or target surface had any effect on the fiber diameters (Figure 9)

All fibers fell within a similar range of approximately 2-5 μm in diameter. Only the low and medium fiber densities for APTES were found to be significantly different with $p = 0.029$. This difference did not have any effect on cell adhesion or spreading (See Chapter 5).

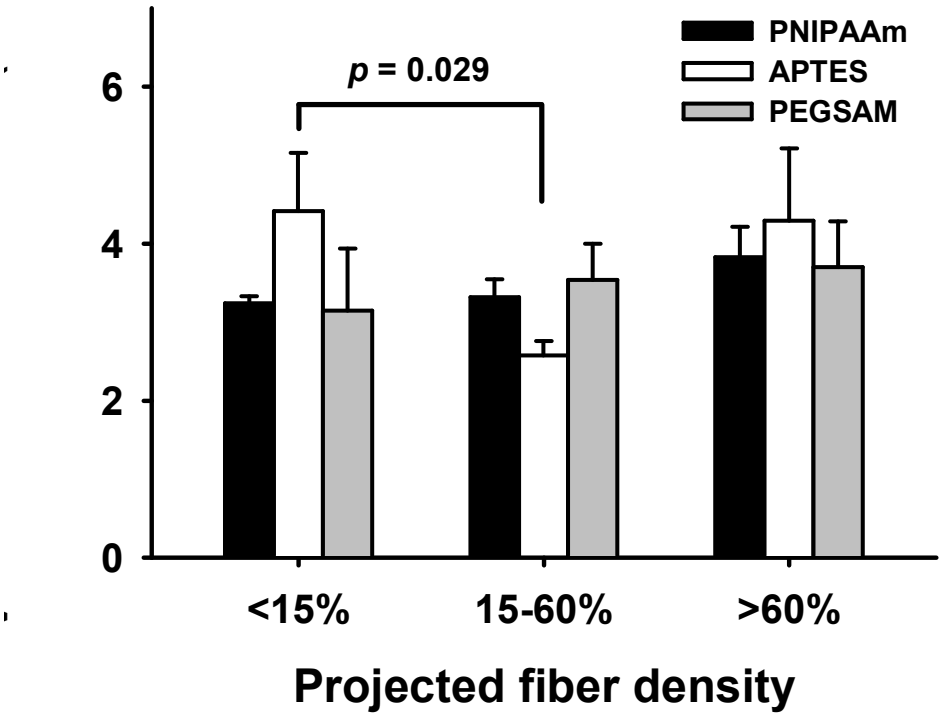

Figure 9: Average fiber diameter as a function of projected fiber density. The only statistically significant difference was between low and medium fiber densities on APTES.

4.4 Conclusions

Microstructure composite surfaces with combined non-adhesive materials were fabricated and characterized. It was possible to incorporate two well characterized surface chemistries, APTES and PEGSAM alongside with PNIPAAm thin film (100 nm) with three different surface topographies provided by electrospun PNIPAAm fibers. The fiber density was classified into low, medium and high projected fiber density bins which corresponded to less than 15% global fiber coverage, 15% - 60% global coverage, and greater than 60% global coverage, respectively. This classification was designated to

provide three scenarios in which the average spacing between fibers was greater than the maximum cell size, greater than the minimally spread cells and less than the cell size. Also, the surface topography incorporated into the microstructure composite surface displayed micron size topography with approximately 2-5 μm in diameter range. The microstructure fabricated will provide a variety of distinctive surface topography and surface chemistries characteristics that will help in conducting cell adhesion studies and elucidate how the adhesivity of surfaces that typically do not support significant cell adhesion may be altered by the presence of topographical features, even if those features are poorly adhesive as well.

CHAPTER 5: CELL ADHESION AND CELL SPREADING ON NON ADHESIVE SURFACES

5.1 Introduction

The manner in which a cell interacts with a biomaterial is largely determined by the physical and chemical nature of the biomaterial surface [14]. It is known, for example, that topography and surface chemistry both affect cellular response in very significant ways [71, 72]. Such cues on their own have provided valuable information such as how to design surfaces that exert control over cell shape [73-76], spreading [77, 78] and adhesion [48, 78-82]. There remains, however, a lack of understanding of the interplay between topography and surface chemistry and the relative impact and contribution of each in modulating cellular behavior [83, 84]. A fundamental understanding of this interplay is necessary to advance biomaterials applications through the design of surfaces that more effectively direct cell function.

The few studies that have looked at the combined effect of surface topography and chemical functionality indicate that cells preferentially respond to one property over the other, but the contribution of each property is not well defined or understood [85-87]. Often the response to combinations cannot be predicted from the individual contributions of each property [88]. For instance, several studies have investigated the relative contribution of mechanical guidance cues with chemical guidance cues (i.e., the effect of topographical patterns versus chemical patterns), and have found that

topographically induced cell alignment often dominates over alignment with chemical patterns, when both are present on the same surface [54, 83, 84, 86, 87, 89-93]. Others have looked at the effect of topographical cues on surfaces of uniform chemical presentation. These reports suggest that while topography can influence cell behavior, the underlying surface chemistry determines the relative influence of the topography [43, 85, 94-103]. Still, no unified principles have emerged that explain the relationship between the physical and chemical features of a surface and cell guidance.

Herein, we investigated a curious phenomenon whereby surfaces that typically do not support significant cell adhesion may have their adhesivity altered by the presence of topographical features, even if those features are poorly adhesive as well (See Figure 10). Specifically, smooth poly(N-isopropylacrylamide) (PNIPAAm) thin films or coatings (greater than 30 nm in thickness) have been shown to display poor intrinsic cell adhesion [66], despite the presence of serum proteins [56, 58, 104, 105]. To investigate the role of topography on such coatings, electrospun PNIPAAm fibers (1-5 um diameter) were overlaid on PNIPAAm thin films. Several topographical patterns were developed, spanning from sparse to dense fiber mats, and cell adhesion strongly depended on the relative available areas for attachment on either the fibers or the supporting surface.

To understand the uniqueness of this observation, PNIPAAm fibers were also electrospun onto a surface known to be non-adhesive (self-assembled monolayer of polyethylene glycol (PEGSAM) alkanethiol on gold) or an adhesive coating (3-aminopropyltriethoxysilane (APTES) on glass) to assess the effect of topographical cues on cellular responses to chemistries with well-characterized, disparate adhesive

properties. Cell adhesion and spreading were enhanced on PEGSAM surfaces by the presence of fibers up to a threshold density; and the highest fiber densities reduced adhesion on APTES and PEGSAM coatings. Most significantly, the combination of PNIPAAm fibers on PEGSAM surfaces, despite both materials being non-adhesive alone, was able to produce cell attachment and spreading similar to the strongly adhesive APTES surfaces. Together these findings point to the complex synergy between surface chemistry and physical structure. This unique experimental design provides new clues as to how cells adapt to their environment and also suggests new dimensions of biomaterial design for fine-tuning cellular control.

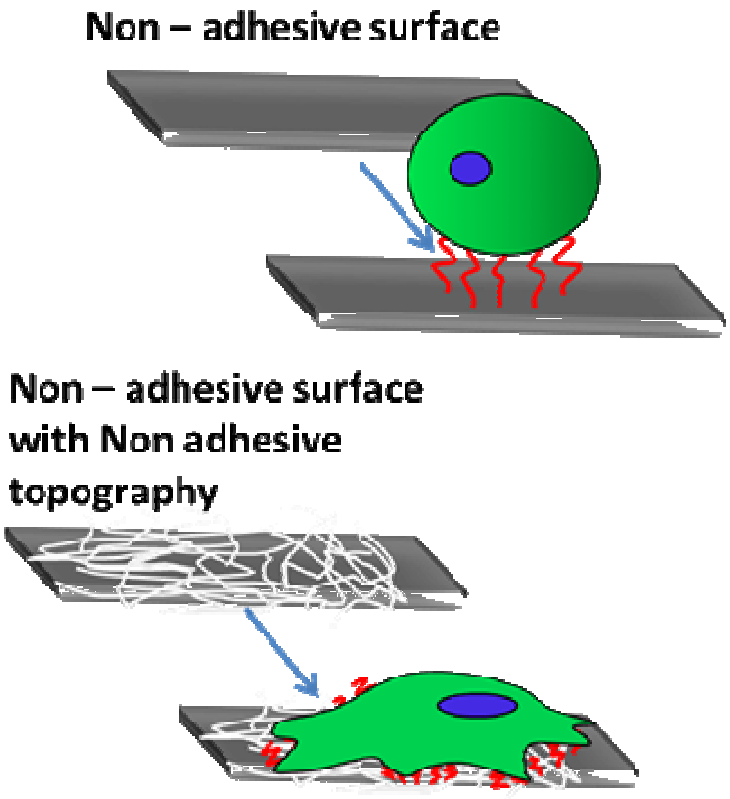

Figure 10: Non-adhesive surface with non-adhesive surface topography

5.2 Materials and Methods

5.2.1 Cell Culture and Reagents

Dulbecco's modified Eagle's medium (Invitrogen, Carlsbad, CA) supplemented with 10% new born calf serum (Invitrogen) and 1% penicillin-streptomycin (Invitrogen) was used as complete growth media (CGM). Cell culture reagents, including human plasma fibronectin and Dulbecco's phosphate-buffered saline (DPBS), Hoechst-33242 and rhodamine-conjugated phalloidin were purchased from Invitrogen. NIH3T3 mouse embryonic fibroblasts (American Type Culture Collection, Manassas, VA) were cultured in CGM on tissue culture polystyrene. Cells were passaged every other day and used between passages 5 and 20. For experiments, cells were enzymatically lifted from the culture dish using trypsin-EDTA (Invitrogen) and then seeded onto the substrates at a density of 100 cell/mm^2 in CGM.

5.2.2 Imaging and Analysis

After incubating the cells on the substrates for 4h, the cells were rinsed in DPBS (Dulbecco's phosphate buffered saline) and the adherent cells were fixed in 3.7% formaldehyde, permeabilized with 0.1% Triton X-100, and stained with Hoechst dye to identify the nucleus and rhodamine-phalloidin to identify actin filaments. The number of adherent cells was counted at specific positions using a Nikon eclipse Ti-U fluorescent microscope (Nikon Instruments, Melville, N.Y.) fitted with a motorized stage and NIS-Elements Advanced Research software (Nikon Instruments) to obtain cell attachment quantification. A thresholding algorithm was utilized to create binary masks of cell boundaries to quantify cell spreading area.

5.2.3 Statistical Analysis

Experiments were performed in triplicate in at least three independent experiments. Data were reported as mean ± SD, and statistical comparisons using SigmaPlot 11 (Systat Software, San Jose, CA) were based on analysis of variance and the Holm-Sidak test for pairwise comparisons, with a p-value < 0.05 considered significant.

5.3 Results

5.3.1 Topographic Enhancement of Cell Adhesion to PNIPAAm

This study arose from the desire to assess the interplay between surface topography and surface chemistry on cell-material adhesion properties. We investigated surfaces with topographical features that were generated from materials that were either the same or different from the underlying surface. In all cases, mouse embryonic fibroblast cells were seeded onto the substrates at a density of 100 cell/mm^2 in CGM and incubated for 4 h in culture medium prior to assessing adhesion. We were motivated to investigate this by the initial observation that fiber-based topographical features enhanced cell adhesion to PNIPAAm (Figure 11).

Cell attachment on smooth 100 nm thick cross-linked PNIPAAm thin films was minimal compared to plain glass controls, demonstrating that these uniform films are not suitable for cell adhesion. However, when the PNIPAAm thin films were overlaid with PNIPAAm fibers of similar composition, cell adhesion was enhanced approximately 20-fold. There was a statistical difference between the smooth 100 nm thick cross-linked PNIPAAm thin films and both the control samples and smooth 100 nm thick cross-linked

PNIPAAm thin films with 30% fiber coverage. No statistical difference was observed between the control samples and the smooth 100 nm thick cross-linked PNIPAAm thin film with 30% fiber coverage samples. This result suggests topography alone may be able to induce adhesion on poorly adhesive materials.

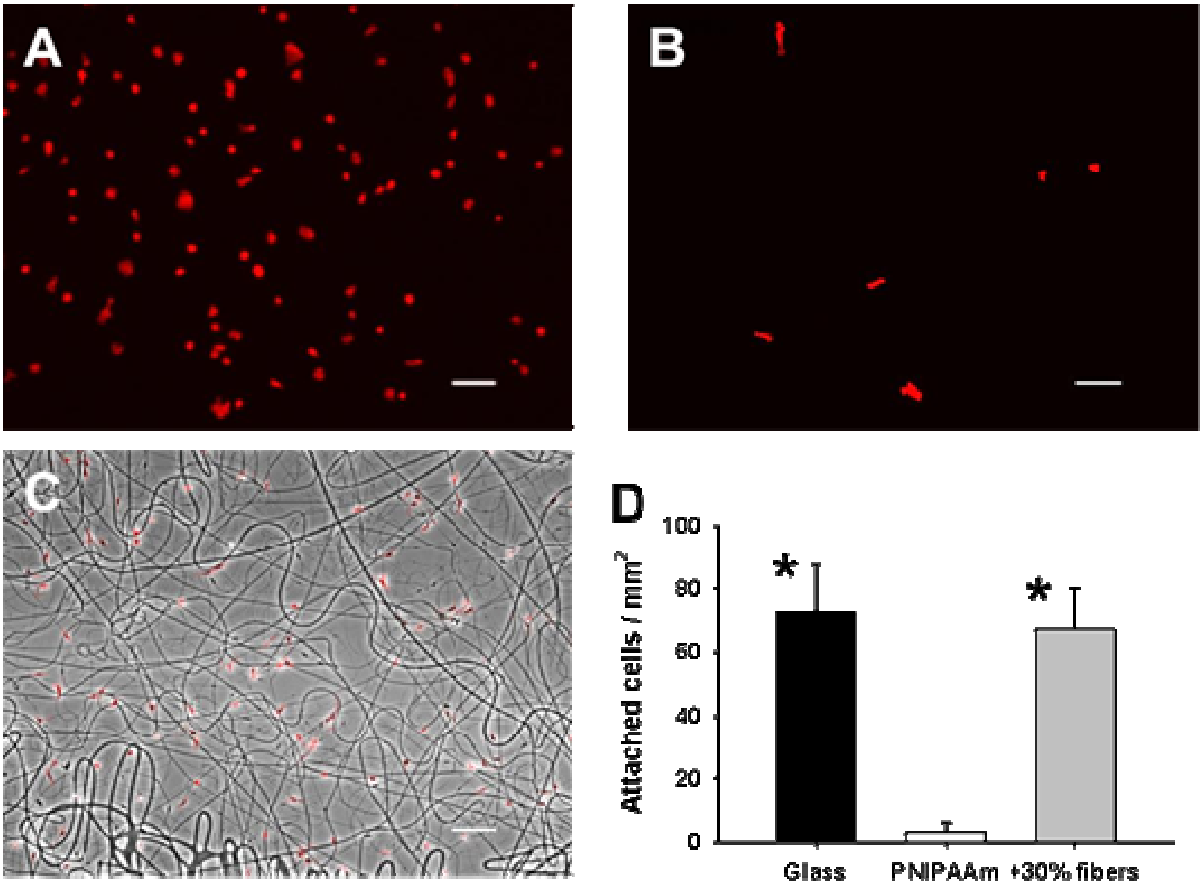

Figure 11: Cell adhesion on (A) glass, (B) PNIPAAm film and (C) PNIPAAm film covered with electrospun PNIPAAm fibers (~30% fiber density) substrates. Approximately 100 cell/mm^2 were seeded on the substrates and incubated for 4h before (D) quantification with fluorescence microscopy. * indicates $p < 0.05$ compared to the smooth PNIPAAm film. (bars = 100 μm)

5.3.2 Cell Adhesion on PNIPAAm, APTES and PEGSAM Surfaces with Varied Fiber Densities

The number of adherent cells following 4 hours in CGM was quantified at specific positions on each substrate (Figures 12 and 13). We first analyzed the trends of cell attachment dependence on fiber density for each underlying surface chemistry. Then we considered the differences between the three surface chemistries for each fiber density.

5.3.2.1 PNIPAAm

Cell adhesion on a bare PNIPAAm film with 0% fiber density was not supported with a low number of cells adhered (<10 cells/mm²). This result is in agreement with other studies done on a bare PNIPAAm surface [56, 58] and consistent with our initial observations (Figure 11). However, cell adhesion was enhanced by the incorporation of PNIPAAm fibers onto the PNIPAAm surface, and cell adhesion was maximum on the medium fiber density (approximately 60 cells/mm^2). No statistical differences were observed among low, medium and high fiber densities; on the other hand, there was a significant difference between bare PNIPAAm films and medium PNIPAAm fiber density on PNIPAAm films.

5.3.2.2 APTES

As expected, cell adhesion was highly supported on the APTES control sample with 0% fiber density, comparable to or greater than on plain glass controls. Cell adhesion was similarly supported on low (<15%) and medium (15%-60%) fiber coverages, indicating that cell adhesion was not affected by the non-adhesive

topographical features. However, by increasing fiber density above 60%, cell adhesion was reduced by about 50%.

5.3.2.3 PEGSAM

Negligible cell adhesion was observed on the uniform PEGSAM surface (0% fiber density). The few cells that adhered to this surface can likely be attributed to defects in the gold or SAM layers. Similar to the PNIPAAm substrates, the incorporation of PNIPAAm fibers on the PEG surfaces significantly enhanced cell adhesion with maximum cell attachment occurring on the medium fiber density (approximately 85 cells/mm^2). Cell adhesion was significantly greater on all fiber densities compared to PEGSAM with no fibers.

5.3.2.4 Comparison of PNIPAAm, PEGSAM and APTES for Each Fiber Density

Cell adhesion on the topographically featureless control samples, denoted as 0% fiber density, was markedly different between the APTES surface and the two other surfaces. This amine-functional surface exhibited complete cell attachment compared to the cell seeding density of approximately 100 cells/mm². However, PNIPAAm and PEGSAM supported minimal cell adhesion (<10 cells/mm²). These adhesive properties were consistent with our expectations based on previous reports. For the low projected fiber density (<15%), cell adhesion on APTES was maximal, while improved but intermediate levels of cell attachment were observed for PNIPAAm and PEGSAM. On medium fiber density (15%-60%), cell adhesion was comparable for APTES and PEGSAM with an average of 80-90 cells/ mm² while PNIPAAm was slightly less (approximately 60 cells/mm²). There were no significant differences among the three

surfaces. For high fiber density (>60%), cell adhesion was reduced overall to approximately 45 cells/mm² for all surface chemistries.

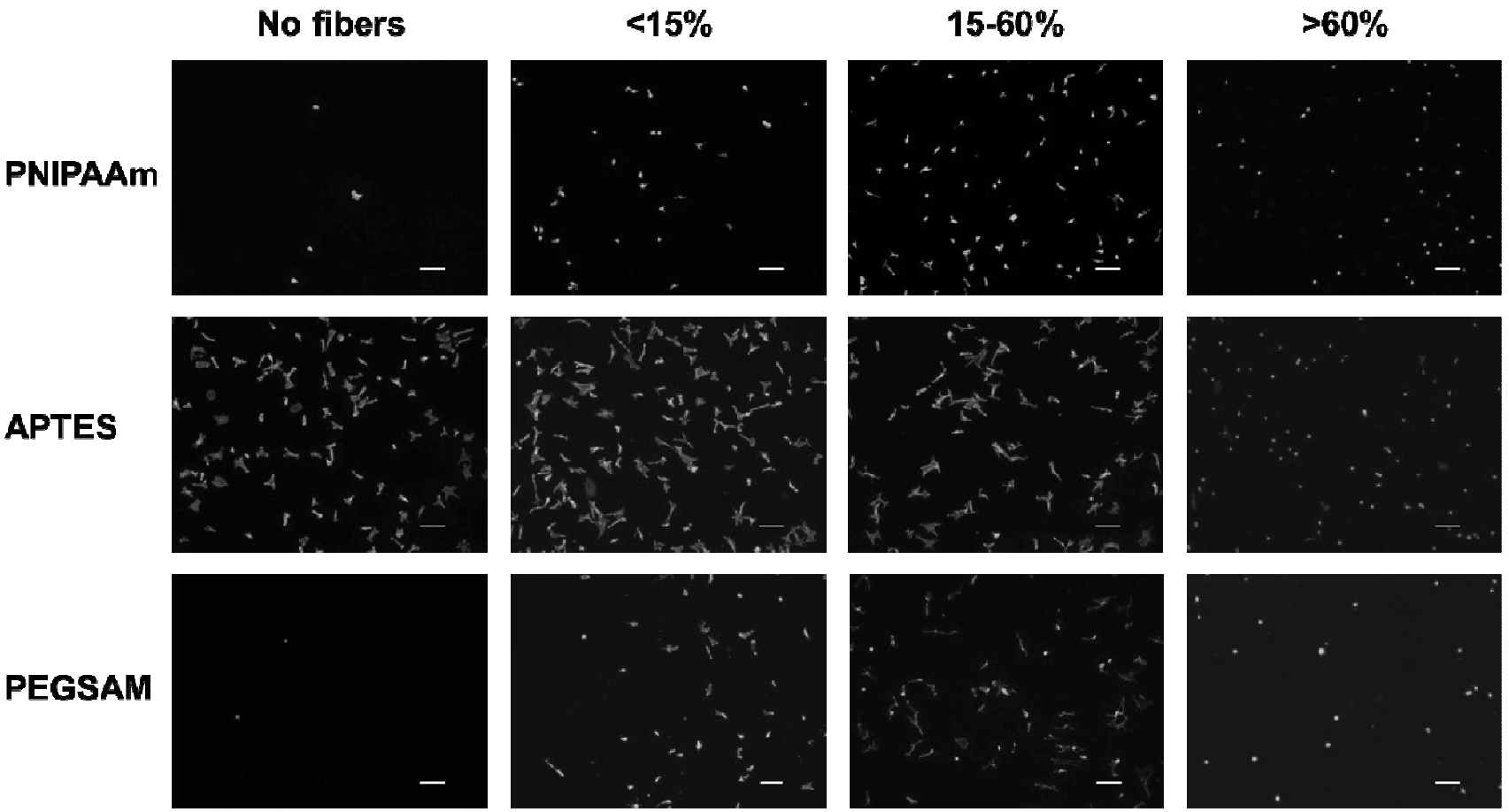

Figure 12: Fluorescence images of attached cells for all the underlying surface chemistries and fiber densities. (bars=100 μm)

.

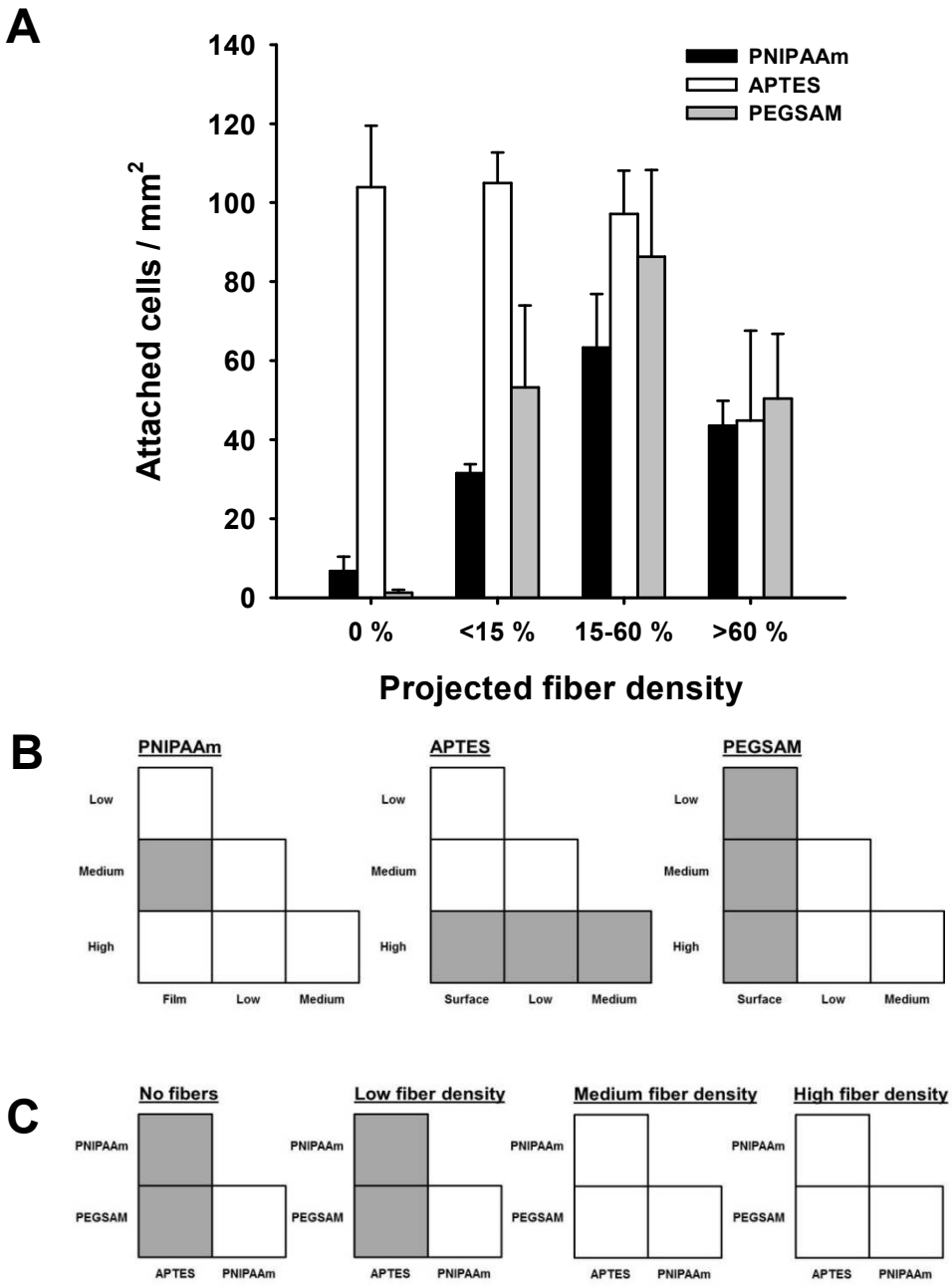

Figure 13: (A) Cell adhesion on low (<15%), medium (15-60%) and high PNIPAAm fiber density (>60%) with PNIPAAm, APTES and PEGSAM underlying surface chemistry. Cells were seeded on the substrates with a cell density of 100 cells/mm^2 and incubated for 4h. (B) Statistical comparisons for cell adhesion for the three binned fiber densities on each individual underlying surface chemistry. (C) Statistical comparisons of cell attachment among surface chemistries for each fiber density. Significant differences were identified by using ANOVA and the Holm-Sidak test for pairwise comparisons, with a p-value < 0.05 considered significant (indicated by the shaded boxes).

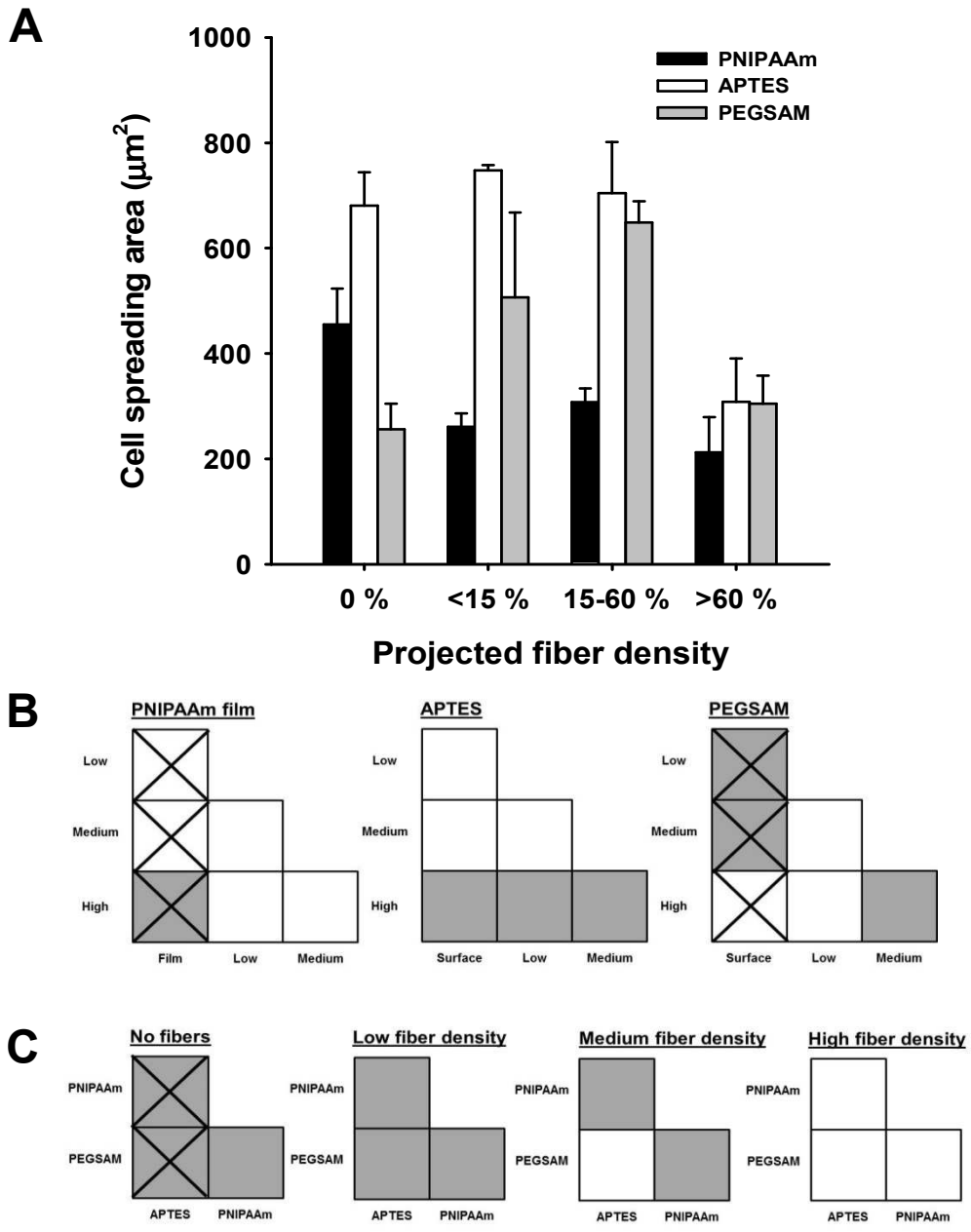

Figure 14: (A) Cell spreading on low (<15%), medium (15-60%) and high PNIPAAm fiber density (>60%) with PNIPAAm, APTES and PEGSAM underlying surface chemistry. Cells were seeded on the substrates with a cell density of 100 cells/mm^2 and incubated for 4h. (B) Statistical comparisons for cell spreading for the three binned fiber densities on each individual underlying surface chemistry. (C) Statistical comparisons of cell spreading among surface chemistries for each fiber density. Significant differences were identified by using ANOVA and the Holm-Sidak test for pairwise comparisons, with a p value < 0.05 considered significant (indicated by the shaded boxes). Crossed out boxes indicate low cell density (<10 cell/mm^2).

5.3.3 Cell Spreading on PNIPAAm, APTES and PEG Surfaces with Varied Fiber Densities

The extent of cell spreading was also analyzed for the attached cells by quantifying the projected cell areas for each substrate and fiber density combination. The results were analyzed with similar comparisons among the fiber densities and surface chemistries as described above (Figure 14).

5.3.3.1 PNIPAAm

Despite the previously described enhancement to cell attachment, cell spreading on low, medium and high PNIPAAm fiber densities upon an underlying PNIPAAm film was not enhanced. Although a statistical difference was observed when the uniform PNIPAAm control substrate was compared to low, medium and high fiber densities it needs to be specified that these comparisons were to a PNIPAAm surface with a very small number of adherent cells (<10 cells/mm²). Thus it is an unreliable comparison. The spreading on fiber-laden PNIPAAm films was minimal with attached cells remaining highly rounded.

5.3.3.2 APTES

Cells spread to a robust 700-750 μm² average area on low and medium fiber density samples coated with APTES. This behavior was comparable to the uniform APTES controls with fibers. Interestingly, for high fiber surface coverage, cell spreading area was reduced to an average of approximately 300 μm².

5.3.3.3 PEG

In contrast to the PNIPAAm surfaces, the incorporation of fibers on the PEGSAM treated surfaces showed that cell spreading could also be supported and enhanced on a non-adhesive surface. On low and medium fiber densities, cell spreading was enhanced reaching a maximum of nearly 700 μm² on the medium fiber coverage, showing that a topographical change supports cell adhesion and spreading even though the underlying substrate had a non-fouling surface that does not typically support cell attachment or spreading. For a high projected fiber density surface (>60%) cell spreading area was again reduced to about 300μm^2. Statistical differences were observed between the uniform PEG control substrates and the low and medium fiber densities (no fiber controls have few adhered cells), and between the medium and high fiber densities.

5.3.3.4 Comparison of PNIPAAm, PEG and APTES for Each Fiber Density

Uniform control samples, denoted as 0% fiber coverage samples, were included in this study along with a range of fiber densities to investigate the hypothesis that the addition of surface topography indeed had an effect in enhancing cell adhesion and spreading regardless of the underlying surface chemistry. It was observed that for uniform surfaces, cells on the APTES surface spread significantly more than on PNIPAAm and PEGSAM surfaces, though the PNIPAAm and PEGSAM surfaces had few attached cells (<10 cells/mm^2) to analyze for spreading.

More importantly, the addition of PNIPAAm fibers to the three surface chemistries influenced cell spreading area differently within each projected fiber density

group. For the low projected fiber density (<15%) group, the APTES surface showed the highest spreading area. Surprisingly, cell spreading area was enhanced for PEGSAM compared to the control while on the PNIPAAm it was not. All three samples were statistically different. On the medium fiber densities (15%-60%), cell spreading remained high on the APTES and low on the PNIPAAm, similar to the low fiber coverage. However the cell spreading area on PEGSAM was enhanced to the level of the APTES (approximately 700 μm^2). For the highest projected fiber density fiber mats (>60%), cell spreading area was minimal for all three surface chemistries. In other words, the high fiber density reduced cell spreading to an area equivalent to cells on the PNIPAAm surface, indicating that cell spreading is independent of underlying surface chemistry for the highest density fiber mats.

5.4 Discussion

The complexity of multiple chemical or physical cues can trigger biological responses that are distinct compared to the individual stimuli. This study focused on the interplay of surface chemistry and physical topography as biomaterial regulators of cell behavior in composite materials.

Platforms created by using electrospun nano- or micro-fibers may mimic structurally the extracellular matrix of native tissues and provide cues that regulate cellular survival or tissue regeneration [106]. We used electrospinning to vary the projected surface coverage of the fibers to understand the cellular response to biomaterial surface topographies ranging from two dimensional surfaces (null or low fiber density) to three dimensional fibrous polymer scaffolds that mimic tissue

architecture (high fiber density). Fiber diameter varied over a small range (approximately 2-5 μm); thus, is possible that the observed responses are unique to the fiber size used in this study. Fiber orientation and curvature may play a role in the enhancement of cell adhesion though these parameters were random and unquantifiable in this design. By binning the fiber density into low, medium and high density regions, we focused specifically on the effects of cell-fiber and cell-substrate interactions.

Our findings showed that on non-adhesive surfaces (PNIPAAm, PEGSAM), cell adhesion increased with increasing PNIPAAm fiber density as long as the underlying surface was available (up to 60% fiber coverage). For both the PNIPAAm and the PEGSAM surfaces, cell adhesion occurred primarily at the fiber/surface interface; however, only in the case of the PEGSAM surface did the cells spread significantly along the fiber. The same spreading was not observed for the PNIPAAm surface. At fiber coverages above 60%, cell adhesion on both surfaces decreased and approached approximately only 50% of the theoretical value.

The reason for the localization of the cells at the fiber/surface interface most likely results from the ability of cells to sense and respond to curvature [107, 108]. Curvature in the cell membrane can localize integral membrane proteins, and it has been shown that membrane scaffolding proteins, such as the Bin–amphiphysin–Rvs (BAR) and epsin N- terminal homology (ENTH) domain superfamilies, preferentially bind to highly curved membranes [109-112]. For instance, Fioretta et al. observed that endothelial cells (colony forming cells and mature endothelial cells) were able to sense the changes in the curvature of electrospun fibers due to the change in the size of the

fiber diameter [113]. The endothelial cells responded to the radius by orienting themselves around the fiber, by either developing a cytoskeleton organized circumferentially or aligning the cytoskeleton along the scaffold fiber axis with collagen deposition aligned in the corresponding direction. Similarly, fibers could enhance adhesion at the sites of curvature on poorly adhesive surfaces via bending the membrane in such way that adhesion proteins are aggregated to these sites.

While fibers enhanced adhesion to the poorly adhesive surfaces, the trend was reversed at the highest fiber densities. Furthermore, at the highest fiber densities, cell attachment and spreading on APTES, which strongly supports cell adhesion and spreading [68, 69], decreased to levels similar to the non-adhesive materials. We hypothesize that because the area between the fibers for low and medium fiber densities was comparable to or greater than a cell's projected area, cells were provided sufficient access to the underlying APTES surface chemistry; however, when the fiber surface coverage was increased further, the cells primarily interacted only with PNIPAAm fibers. In other words, the underlying surface chemistry became irrelevant as the area between the fibers shrunk to average sizes smaller than the cells' preferred projected area.

Explaining the significant difference in the cell spreading on fibers between the PEGSAM and PNIPAm surfaces is more challenging because the smooth surfaces similarly repelled cell adhesion. Cell adhesion to synthetic biomaterials is typically mediated by adsorbed proteins [45], and PEGSAM is known to be non-fouling (resistant to protein adsorption) and therefore resistant to cell adhesion except where defects in the SAM occur [114, 115]. On the other hand, proteins readily adsorb to PNIPAAm, and

if virgin PNIPAAm is initially incubated with adhesion molecules such as fibronectin or poly-lysine, cell attachment improves significantly [116]. Perhaps the adsorption of adhesive serum components onto PNIPAAm fibers on the non-fouling PEGSAM creates a chemical heterogeneity that encourages cell spreading. This of course brings up the interesting postulation that while topography can enhance adhesion on weakly adhesive surfaces, chemical heterogeneity is necessary for cell spreading. The mechanism of enhanced spreading on topographical composites may also result from the synergy of the chemical heterogeneity and the aggregation of cell surface proteins due to the membrane bending on the fibers or at the fiber-surface interface.

In summary, these results indicate that smooth non-adhesive materials can be converted to cell adhesive by the addition of topographic features. Moreover, the combination of two different non-adhesive materials in fibrous and planar forms resulted in maximal cell adhesion and spreading. These findings have implications for the fabrication of instructive biomaterials with greater control over cell functions using combinations of surface chemistry, topography and composite materials with contrasting properties. This may also be a significant step toward explaining why cell behavior in 3-dimensional cultures is often different than on simple planar cell supports.

5.5 Conclusions

Micron diameter PNIPAAm micron fibrous scaffolds of low (<15%), medium (15-60%) and high (>60%) density were superimposed on uniform coatings of PNIPAAm, PEGSAM, and APTES in order to investigate the effect of topography on the adhesion and spreading on embryonic fibroblast cells. The investigation revealed a complex

interplay between chemical and physical clues, especially an unexpected synergism between two disparate and non-adhesive material surfaces. Surprisingly, the PEGSAM surface with a medium density mat of PNIPAAm fibers was statistically equivalent to the APTES surface with regards to both the fraction of adhered cells and the area of cell spreading. The disparate material phases are critical. The PNIPAAm surface with a medium density PNIPAAm had no statistical effect on spreading although it did enhance cell attachment density compared to the smooth PNIPAAm surface. These results point to not only the effect of topography of non-adhesive surfaces (which enhances cell adhesion in comparison to smooth surfaces), but how chemical dissimilarity between two non-adhesive materials can stimulate cell spreading. Taken in aggregate, these findings could motivate the design of new composite biomaterials that regulate cell adhesion and other functions.

CHAPTER 6: CELL ADHESION AND SPREADING RESPONSE ON PHOTO-CROSSLINKED PNIPAAm THIN FILM COATINGS

6.1 Introduction

As already stated in the background section (Chapter 2) surface topography plays a major role in modulating cellular behavior. Topography can be intentionally created or by accident and in both cases topography can vary from a macro to a nanometer scale. At the macromolecular level a surface may appear to be smooth, but in fact if the surface is looked at a microscale or nanoscale level the surface may not appear to be smooth anymore, displaying some type of topography. The scale of the topography present on a biomaterial can have a strong effect in modulating cellular response influencing the physicochemical interactions central to biological processes that involve proteins and cells. Macro and micron scale topography have been extensively studied showing that chemical functionality and topography have a strong effect over cell shape, spreading and adhesion [117]. However, there is less knowledge about how cells react to nanoscale topography. However, cells are prone to react to nanostructures due to the in vivo characteristics of their surrounding microenvironments. For example, the extracellular matrix (ECM), the protein matrix surrounding cells in tissues, contains collagen fibrils that are of nanometer scale and the cell's own surface is organized on the nanoscale level, including receptors and filopodia [118, 119]. For instance, bone tissue contains an array of collagen type I fibrils with a spacing of 68 nm between fibers and 35 nm in depth [120].

This study was motivated by the work that we presented in Chapter 5 as well as work published by other groups that showed that cell adhesion was enhanced on PNIPAAm film with a thickness < 30 nm [66]. They believe that cell enhancement is due to the reduction in thickness of PNIPAAm film layer. We hypothesized that this cell adhesion enhancement is actually a result of nanoscale topography on the surface of the PNIPAAm film. That surface topography is likely a function of the topography of the underlying substrate. We report preliminary results on cell adhesion on various thickness films of PNIPAAm coated on polystyrene petri dishes and glass cover slips which have different topographies (roughness). Polystyrene petri dishes and glass cover slips (borosilicate) were chosen for this study because they have different roughness properties. It has been reported that the roughness of polystyrene petri dishes varies depending on the brand between 1.5 nm to 6.5 nm. In this study we are using Corning and the roughness corresponding to this brand is ~3.5 nm. For borosilicate glass cover slips the roughness has been reported to be between approximately 0.2 nm – 1.0 nm. We hypothesized that the surface roughness of the support and the thickness of the PNIPAAm film can modulate the adhesive properties of the film. The preliminary results suggest that the adhesive properties of this material are enhanced and it showed a dependence on the roughness of the support and the thickness of the film. To complete this study, we need to do further experiments (n=3) and use AFM imaging to characterize the PNIPAAm films for both types of surfaces.

6.2 Materials and Methods

6.2.1 Substrate Preparation

Two types of substrates were used; round glass cover slips and polystyrene petri dishes (25 mm). The glass cover slips were sonicated in ethanol for 15 minutes, blown dry with a stream of nitrogen gas and oxygen plasma cleaned. No cleaning method was used for the polystyrene petri dishes. The glass cover slip substrates were submerged in a solution of 1.0 v/v% 3-aminopropyltriethoxysilane for 15 minutes, rinsed with acetone and dried at 110ºC for 10 minutes [55, 68, 69].

PNIPAAm thin films were prepared following the protocol reported by Maria E. Nash et al. [66]. A 300 mL aliquot of PNIPAAm in ethanol solution (0.125 wt %, 0.25 wt %, 0.5 wt % and 3 wt %) was deposited onto the petri dishes and the APTES treated glass substrate to a slowly spinning substrate. The PNIPAAm solution was initially deposited onto each substrate at a speed of 150 rpm, followed by a high speed of 6000 rpm for 30s. The substrate with the polymer film was cross-linked by UV light (365 nm) for 30 min. Film thickness was assessed by ellipsometry [65].

6.2.2 Cell Culture and Reagents

Dulbecco's modified Eagle's medium (Invitrogen, Carlsbad, CA) supplemented with 10% new born calf serum (Invitrogen) and 1% penicillin-streptomycin (Invitrogen) was used as complete growth media (CGM). Cell culture reagents, including human plasma fibronectin and Dulbecco's phosphate-buffered saline (DPBS), Hoechst-33242 and rhodamine-conjugated phalloidin were purchased from Invitrogen. NIH3T3 mouse embryonic fibroblasts (American Type Culture Collection, Manassas, VA) were cultured

in CGM on tissue culture polystyrene. Cells were passaged every other day and used between passages 5 and 20. For experiments, cells were enzymatically lifted from the culture dish using trypsin-EDTA (Invitrogen) and then seeded onto the substrates at a density of 100 cell/mm^2 in CGM.

6.2.3 Imaging and Analysis

After incubating the cells on the substrates for 4h, the cells were rinsed in DPBS (Dulbecco's phosphate buffered saline) and the adherent cells were fixed in 3.7% formaldehyde, permeabilized with 0.1% Triton X-100, and stained with Hoechst dye to identify the nucleus and rhodamine-phalloidin to identify actin filaments. The number of adherent cells was counted at specific positions using a Nikon eclipse Ti-U fluorescent microscope (Nikon Instruments, Melville, N.Y.) fitted with a motorized stage and NIS-Elements Advanced Research software (Nikon Instruments) to obtain cell attachment quantification.

6.2.4 Statistical Analysis

The preliminary results shown in this section correspond to one experiment for each substrate type. Once the experiments are completed, (n=3) which means that experiments will be performed in triplicate in at least three independent experiments, data will be reported as mean ± SD, and statistical comparisons using SigmaPlot 11 (Systat Software, San Jose, CA) will be based on analysis of variance and the Holm-Sidak test for pairwise comparisons, with a p-value < 0.05 considered significant.

6.3 Results

6.3.1 Topographic Enhancement of Cell Adhesion to PNIPAAm Thin Films

A range of PNIPAAm film thicknesses was created by varying the polymer concentration while keeping the spin coating recipe constant. The thickness for films formed from each PNIPAAm solution concentration was measured by ellipsometry and the results are reported in Table 2. The number of adherent cells following 4 hours in CGM was quantified at specific positions on each substrate (Figures 15 and 16). We first analyzed the trends of cell attachment dependence on PNIPAAm film thickness for each type of substrate and compared them to cell attachment on the controls substrates, bare glass and polystyrene petri dish. Then we considered the differences between the petri dishes and glass cover slips. The results reported in this section are preliminary results and further experiments will be conducted to support data and a statistical analysis will be executed.

6.3.1.1 Polystyrene Petri Dish Film Supports

Preliminary results suggest that cell adhesion and spreading is enhanced as PNIPAAm film thickness is reduced. PNIPAAm film with a thickness of 158 nm exhibits a minimal cell adhesion (<10 cells/mm^2). The non-adhesive property for this thickness was consistent with our expectations based on previous reports. Cell adhesion on the PNIPAAm films with thicknesses 7 nm, 10 nm and 20 nm was enhanced, and it is equivalent to the control sample.

6.3.1.2 Glass Cover Slip Film Supports

Similarly, PNIPAAm films with a thickness of 158 nm exhibits minimal cell adhesion (<10 cells/mm²) upon a glass support and this is consistent with previous reports. Preliminary results suggest that cell adhesion is only slightly enhanced for PNIPAAm films in the 10-20nm range, and reached maximum attachment on 7 nm thick films.

6.3.1.3 Comparison of Petri Dish with Glass Cover Slip Underlying Film Supports

Cell adhesion on both petri dish and glass cover slip control samples showed similar cell adhesion, and it compared to the cell seeding density of approximately 100 cells/mm². For the samples with high thickness (158 nm), both surfaces showed minimal cell adhesion (<10 cells/mm^2) and the values were similar to each other. There is a marked contrast in cell adhesion between the petri dish and the glass cover slip samples with PNIPAAm film thickness of 10 nm and 20 nm. In both cases cell adhesion levels on glass cover slip, were lower (intermediate levels) when compared to the petri dish values. Cell adhesion on the thinnest PNIPAAm film (7nm) was greatly enhanced for the glass cover slip sample and the value was comparable to the number of cells attached on the petri dish sample.

Table 2: PNIPAAm thickness (nm)

PNIPAAm Solution Concentration (wt %)	Thickness (nm)
0.125	7
0.25	10
0.5	20
3	158

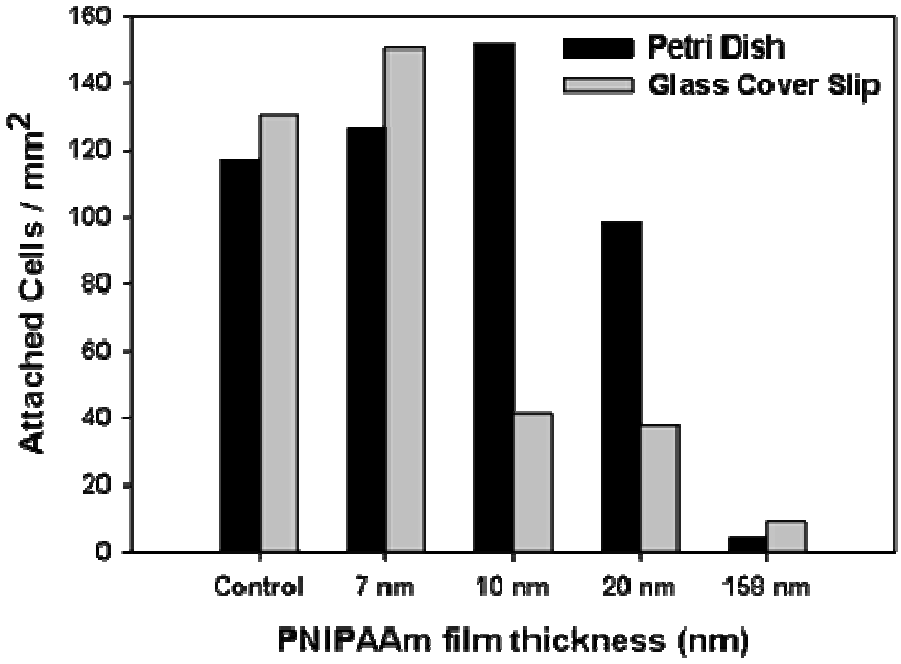

Figure 15: Cell adhesion on PNIPAAm films. Cells were seeded on the substrates with a cell density of 100 cells/mm^2 and incubated for 4h.

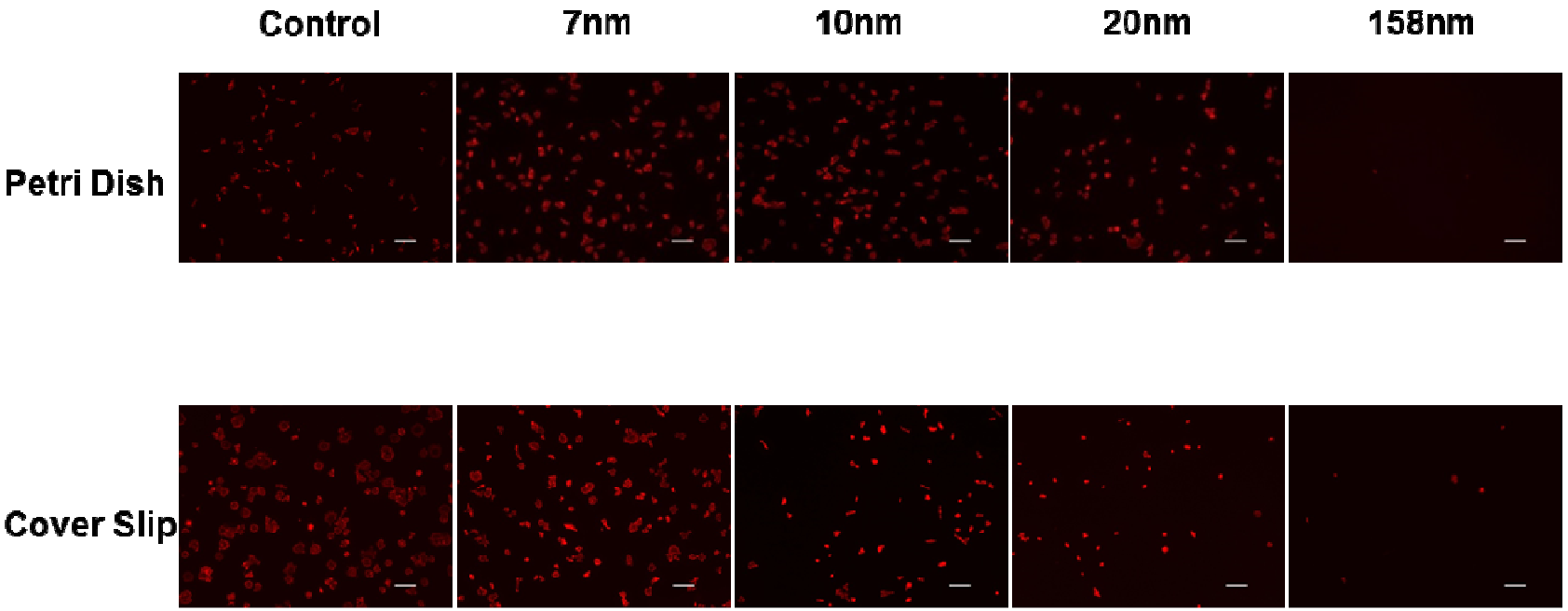

Figure 16: Fluorescence images of attached cells on PNIPAAm thin films with petri dish and glass cover slip underlying film supports (bars=100 μm)

6.4 Discussion

To test the hypothesis that nanoscale topography can enhance cell adhesion on PNIPAAm thin films, we prepared PNIPAAm thin films with controlled thickness by varying the concentration of the solution deposited during the spin coating process. Our preliminary results suggest that cell adhesion increased as the PNIPAAm film thickness decreased, with a minimal cell attachment on PNIPAAm films with thickness of 158 nm. Cell adhesion was markedly enhanced on both petri dish and glass cover slip on the 7nm PNIPAAM thin film samples. Even though we see a contrast on cell attachment between petri dishes and glass cover slips, within the same thickness group we can say that cell adhesion was enhanced and there is a threshold in PNIPAAm thickness in which PNIPAAm adhesive properties are modulated.

To further understand and support our hypothesis we need to complete at least three experiments for each condition (n=3). Also, Atomic Force Microscopy Imaging and surface roughness measurements would be a suitable way to obtain information about the surface topography of the films to support our hypothesis.

6.5 Conclusions

We believe that the adhesivity of PNIPAAm thin films is modulated by nanoscale topography present on the surface of the PNIPAAm layer. Thick films will be smooth while the surface topography becomes more similar to the underlying support as the thickness of the PNIPAAm film decreases. Further experiments are expected to support this hypothesis that the transition from non-adhesive to adhesive for PNIPAAm is triggered by the presence of nanoscale topography. Cells may sense this topography by

changes in protein adsorption or local curvature in their membranes [109-112, 121, 122]. Whatever the mechanism, this topographic effect explains the dependence of cell adhesion to PNIPAAm on film thickness which cells cannot directly sense.

CHAPTER 7: CONCLUSIONS AND FUTURE WORK

7.1 Conclusions

The key findings in this dissertation are summarized as follows:

1. A stable and reproducible microstructure with combined topography and surface chemistry of non-adhesive materials was successfully fabricated for cellular response studies.

2. Adhesive properties of non-adhesive materials were enhanced by the presence of microscale topography, even when the material used to create the topography was poorly adhesive as well.

3. The electrospun fiber density that created the microscale topography showed a thresholding factor (>60%) independent of the underlying surface chemistry, in which cell adhesion and spreading was no longer supported.

4. Medium fiber density (15% - 60%) with PEGSAM underlying surface chemistry showed cell adhesion enhancement similar to the APTES adhesive coating and cell seeding density (100 cells/mm^2).

5. Low and medium fiber density on PNIPAAm thin film layer (100nm) enhanced cell adhesion but cell spreading response was minimal; and unchanged.

6. Preliminary results of cell adhesion on PNIPAAm thin film layers, spin coated on petri dishes and glass cover slip is enhanced as the thickness of the film is reduced.

7. Cell adhesion on the thickest PNIPAAm film for both petri dish and glass cover slip was minimal and in agreement with previously reported results

8. PNIPAAm films spin coated on petri dishes showed higher cellular response when compared to the same PNIPAAm film thicknesses spin coated on glass cover slips.

9. Further experiments will support preliminary results showing that nanoscale topography enhances cell adhesion on PNIPAAm thin film and not the film thickness.

Physical properties of the surface of PNIPAAm, a poorly adhesive material under many conditions, can modulate cell adhesion. We observed that topographic features in the form of overlaid micron scale fiber mats or nanoscale textures supporting thin films were able to support cell adhesion similar to highly adhesive materials. In contrast, smooth films repelled cell adhesion. It was shown that there is a dependence on the fiber density of the overlaid micron fiber PNIPAAm mats and the PNIPAAm film thickness (higher the thickness the smother the film becomes) in the adhesive properties of PNIPAAm. A fiber density below 60% of overlaid micron scale fiber mats on a non-adhesive material enhanced the adhesive properties of the material, showing maximum enhancement when the materials are of different surface chemistries. As for the PNIPAAm films, it was shown that the underlying roughness of the supporting

material affect the adhesive properties of PNIPAAm film differently depending on the thickness of the film. The roughness of the substrate used, can modulate and enhance the adhesive properties of a poorly adhesive material to some extent. A combination of the substrate roughness and the film thickness can exert control over cell adhesion.

It can be concluded that surface topography matters, and it can enhance the adhesive properties of a poorly adhesive material comparable to an adhesive surface. By controlling the substrate used, the PNIPAAm film thickness and the fiber density of the overlaid fiber PNIPAAm mats cell adhesion can be modulated. These results will help in the design of new biomaterials that required control over cell adhesion properties.

7.2 Future Directions

The proposed work will help elucidate some of the findings within this work.

1. Evaluate the mechanism that promotes cell adhesion on non-adhesive materials

    a. Quantification of protein adsorption on PNIPAAm electrospun fibers.

2. Evaluate cell adhesion enhancement on PNIPAAm thin films

    a. Further experiments on both type of surfaces, petri dish and glass cover slip will support the preliminary results.

    b. Statistical analysis will be done to show any difference between the two types of surfaces and within each group.

3. Atomic force microscopy (AFM) will provide qualitative and quantitative information regarding PNIPAAm surface topography (roughness).

REFERENCES

1. Gattazzo, F., A. Urciuolo, and P. Bonaldo, *Extracellular matrix: A dynamic microenvironment for stem cell niche().* Biochimica et Biophysica Acta, 2014. **1840**(8): p. 2506-2519.
2. Anselme, K., L. Ploux, and A. Ponche, *Cell/Material Interfaces: Influence of Surface Chemistry and Surface Topography on Cell Adhesion.* Journal of Adhesion Science and Technology, 2010. **24**(5): p. 831-852.
3. Anderson, J.M., A. Rodriguez, and D.T. Chang, *FOREIGN BODY REACTION TO BIOMATERIALS.* Seminars in immunology, 2008. **20**(2): p. 86-100.
4. Navarro, M., et al., *Biomaterials in orthopaedics*. Vol. 5. 2008. 1137-1158.
5. Burkert, S., et al., *Protein Resistance of PNIPAAm Brushes: Application to Switchable Protein Adsorption.* Langmuir, 2010. **26**(3): p. 1786-1795.
6. Akiyama, Y., et al., *Ultrathin poly(N-isopropylacrylamide) grafted layer on polystyrene surfaces for cell adhesion/detachment control.* Langmuir, 2004. **20**(13): p. 5506-11.
7. Fukumori, K., et al., *Temperature-responsive glass coverslips with an ultrathin poly(N-isopropylacrylamide) layer.* Acta Biomater, 2009. **5**(1): p. 470-6.
8. Fukumori, K., et al., *Characterization of Ultra-Thin Temperature-Responsive Polymer Layer and Its Polymer Thickness Dependency on Cell Attachment/Detachment Properties.* Macromolecular Bioscience, 2010. **10**(10): p. 1117-1129.

9. Canavan, H.E., et al., *Surface characterization of the extracellular matrix remaining after cell detachment from a thermoresponsive polymer.* Langmuir, 2005. **21**(5): p. 1949-55.

10. Canavan, H.E., et al., *Comparison of Native Extracellular Matrix with Adsorbed Protein Films Using Secondary Ion Mass Spectrometry.* Langmuir, 2007. **23**(1): p. 50-56.

11. Xue, C., et al., *Protein Adsorption on Poly(N-isopropylacrylamide) Brushes: Dependence on Grafting Density and Chain Collapse.* Langmuir, 2011. **27**(14): p. 8810-8818.

12. Williams, D.F., *The Williams Dictionary of Biomaterials*. 1999, Liverpool: Liverpool University Press.

13. Roach, P., et al., *Modern biomaterials: a review—bulk properties and implications of surface modifications*. 2007, Springer Netherlands. p. 1263-1277.

14. Hubbell, J.A., *Biomaterials in Tissue Engineering.* Nat Biotech, 1995. **13**(6): p. 565-576.

15. Chan, B.P. and K.W. Leong, *Scaffolding in tissue engineering: general approaches and tissue-specific considerations.* European Spine Journal, 2008. **17**(Suppl 4): p. 467-479.

16. Kirchhof, K. and T. Groth, *Surface modification of biomaterials to control adhesion of cells.* Clin Hemorheol Microcirc, 2008. **39**(1-4): p. 247-51.

17. Bacakova, L., et al., *Cell adhesion on artificial materials for tissue engineering.* Physiol Res, 2004. **53 Suppl 1**: p. S35-45.

18. Cook, A.D., et al., *Characterization and development of RGD-peptide-modified poly(lactic acid-co-lysine) as an interactive, resorbable biomaterial.* J Biomed Mater Res, 1997. **35**(4): p. 513-23.

19. Kim, J.H. and S.C. Kim, *PEO-grafting on PU/PS IPNs for enhanced blood compatibility--effect of pendant length and grafting density.* Biomaterials, 2002. **23**(9): p. 2015-25.

20. O'Brien, F.J., *Biomaterials & scaffolds for tissue engineering.* Materials Today, 2011. **14**(3): p. 88-95.

21. Lam, M.T. and J.C. Wu, *Biomaterial applications in cardiovascular tissue repair and regeneration.* Expert review of cardiovascular therapy, 2012. **10**(8): p. 1039-1049.

22. Eun, S.C., *Composite Tissue Allotransplantation Immunology.* Archives of Plastic Surgery, 2013. **40**(2): p. 141-153.

23. Langer, R. and J.P. Vacanti, *Tissue engineering.* Science, 1993. **260**(5110): p. 920-6.

24. Cleveland Clinic, *Treatments and Procedures.* 1995 -2013.

25. Lundbæk, J.A., et al., *Lipid bilayer regulation of membrane protein function: gramicidin channels as molecular force probes.* Journal of The Royal Society Interface, 2010. **7**(44): p. 373-395.

26. Shapiro, L. and W.I. Weis, *Structure and Biochemistry of Cadherins and Catenins.* Cold Spring Harbor Perspectives in Biology, 2009. **1**(3): p. a003053.

27. De Arcangelis, A. and E. Georges-Labouesse, *Integrin and ECM functions: roles in vertebrate development.* Trends in Genetics, 2000. **16**(9): p. 389-395.

28. Schwartz, M.A., *Integrins and extracellular matrix in mechanotransduction.* Cold Spring Harb Perspect Biol, 2010. **2**(12): p. a005066.

29. Gallant, N.D., K.E. Michael, and A.J. García, *Cell Adhesion Strengthening: Contributions of Adhesive Area, Integrin Binding, and Focal Adhesion Assembly.* Molecular Biology of the Cell, 2005. **16**(9): p. 4329-4340.

30. Wilson, C.J., et al., *Mediation of biomaterial-cell interactions by adsorbed proteins: a review.* Tissue Eng, 2005. **11**(1-2): p. 1-18.

31. Berrier, A.L. and K.M. Yamada, *Cell-matrix adhesion.* J Cell Physiol, 2007. **213**(3): p. 565-73.

32. Chou, L., et al., *Substratum surface topography alters cell shape and regulates fibronectin mRNA level, mRNA stability, secretion and assembly in human fibroblasts.* Journal of cell science, 1995. **108**(4): p. 1563-1573.

33. Chai, C. and K.W. Leong, *Biomaterials Approach to Expand and Direct Differentiation of Stem Cells.* Molecular therapy : the journal of the American Society of Gene Therapy, 2007. **15**(3): p. 467-480.

34. Curtis, A. and C. Wilkinson, *Topographical control of cells.* Biomaterials, 1997. **18**(24): p. 1573-1583.

35. Hoffman-Kim, D., J.A. Mitchel, and R.V. Bellamkonda, *Topography, Cell Response, and Nerve Regeneration.* Annual review of biomedical engineering, 2010. **12**: p. 203-231.

36. Biggs, M.J.P., R.G. Richards, and M.J. Dalby, *Nanotopographical modification: a regulator of cellular function through focal adhesions.* Nanomedicine : nanotechnology, biology, and medicine, 2010. **6**(5): p. 619-633.

37. RG., H., *The cultivation of tissues in extraneous medium as a method of morphogenetic study.* Anat Rec., 1912. **6**: p. 181-193.

38. Weiss, P., *The problem of specificity in growth and development.* Yale J Biol Med, 1947. **19**(3): p. 235-78.

39. Charest, J.L., et al. *Polymer cell culture substrates with combined nanotopographical patterns and micropatterned chemical domains*. AVS.

40. Ghibaudo, M., et al., *Substrate Topography Induces a Crossover from 2D to 3D Behavior in Fibroblast Migration.* Biophysical Journal, 2009. **97**(1): p. 357-368.

41. Chew, S.Y., et al., *The effect of the alignment of electrospun fibrous scaffolds on Schwann cell maturation.* Biomaterials, 2008. **29**(6): p. 653-661.

42. Chang, H.-I. and Y. Wang, *Cell Responses to Surface and Architecture of Tissue Engineering Scaffolds*. Regenerative Medicine and Tissue Engineering - Cells and Biomaterials. 2011.

43. Zinger, O., et al., *Differential regulation of osteoblasts by substrate microstructural features.* Biomaterials, 2005. **26**(14): p. 1837-1847.

44. Xu, L.-C. and C.A. Siedlecki, *Effects of surface wettability and contact time on protein adhesion to biomaterial surfaces.* Biomaterials, 2007. **28**(22): p. 3273-3283.

45. Keselowsky, B.G., D.M. Collard, and A.J. García, *Surface chemistry modulates focal adhesion composition and signaling through changes in integrin binding.* Biomaterials, 2004. **25**(28): p. 5947-5954.

46. Keselowsky, B.G., D.M. Collard, and A.J. Garci-a, *Integrin binding specificity regulates biomaterial surface chemistry effects on cell differentiation.* Proceedings of the National Academy of Sciences, 2005. **102**(17): p. 5953-5957.

47. Zhang, M., et al., *Properties and biocompatibility of chitosan films modified by blending with PEG.* Biomaterials, 2002. **23**(13): p. 2641-2648.

48. Llopis-Hernández, V., et al., *Role of Surface Chemistry in Protein Remodeling at the Cell-Material Interface.* PLoS ONE, 2011. **6**(5): p. e19610.

49. Goddard, J.M. and J.H. Hotchkiss, *Polymer surface modification for the attachment of bioactive compounds.* Progress in Polymer Science, 2007. **32**(7): p. 698-725.

50. Zhu, X., et al., *Electrospun Fibrous Mats with High Porosity as Potential Scaffolds for Skin Tissue Engineering.* Biomacromolecules, 2008. **9**(7): p. 1795-1801.

51. Balcells, M. and E.R. Edelman, *Effect of pre-adsorbed proteins on attachment, proliferation, and function of endothelial cells.* Journal of cellular physiology, 2002. **191**(2): p. 155-161.

52. Jäger, M., et al., *Significance of Nano- and Microtopography for Cell-Surface Interactions in Orthopaedic Implants*. 2007.

53. Garcia, A.J., M.D. Vega, and D. Boettiger, *Modulation of Cell Proliferation and Differentiation through Substrate-dependent Changes in Fibronectin Conformation.* Molecular biology of the cell, 1999. **10**(3): p. 785-798.

54. Tan, J. and W.M. Saltzman, *Topographical control of human neutrophil motility on micropatterned materials with various surface chemistry.* Biomaterials, 2002. **23**(15): p. 3215-3225.

55. Vidyasagar, A., J. Majewski, and R. Toomey, *Temperature Induced Volume-Phase Transitions in Surface-Tethered Poly(N-isopropylacrylamide) Networks.* Macromolecules, 2008. **41**(3): p. 919-924.

56. Haraguchi, K., T. Takehisa, and M. Ebato, *Control of Cell Cultivation and Cell Sheet Detachment on the Surface of Polymer/Clay Nanocomposite Hydrogels.* Biomacromolecules, 2006. **7**(11): p. 3267-3275.

57. Selezneva, I.I., A.V. Gorelov, and Y.A. Rochev, *Use of thermosensitive polymer material on the basis of N-isopropylacrylamide and N-tert-butylacrylamide copolymer in cell technologies.* Bulletin of Experimental Biology and Medicine, 2006. **142**(4): p. 538-541.

58. Moran, M.T., et al., *Cell growth and detachment from protein-coated PNIPAAm-based copolymers.* Journal of Biomedical Materials Research Part A, 2007. **81A**(4): p. 870-876.

59. Teo, W.E. and S. Ramakrishna, *A review on electrospinning design and nanofibre assemblies.* Nanotechnology, 2006. **17**(14): p. R89.

60. Bhardwaj, N. and S.C. Kundu, *Electrospinning: A fascinating fiber fabrication technique.* Biotechnology Advances, 2010. **28**(3): p. 325-347.

61. Larsen, G., R. Spretz, and R. Velarde-Ortiz, *Use of Coaxial Gas Jackets to Stabilize Taylor Cones of Volatile Solutions and to Induce Particle-to-Fiber Transitions.* Advanced Materials, 2004. **16**(2): p. 166-169.

62. Wilm, M.S. and M. Mann, *Electrospray and Taylor-Cone theory, Dole's beam of macromolecules at last?* International Journal of Mass Spectrometry and Ion Processes, 1994. **136**(2–3): p. 167-180.

63. *Spin Coating Theory*. 1997 - 2015 [cited 2015 June 18]; Available from: http://www.brewerscience.com/spin-coating-theory.

64. Hall, D.B., P. Underhill, and J.M. Torkelson, *Spin coating of thin and ultrathin polymer films.* Polymer Engineering & Science, 1998. **38**(12): p. 2039-2045.

65. Patra, L. and R. Toomey, *Viscoelastic Response of Photo-Cross-Linked Poly(N-isopropylacrylamide) Coatings by QCM-D.* Langmuir, 2010. **26**(7): p. 5202-5207.

66. Nash, M.E., et al., *Ultra-thin spin coated crosslinkable hydrogels for use in cell sheet recovery-synthesis, characterisation to application.* Soft Matter, 2012. **8**(14): p. 3889-3899.

67. Lannutti, J., et al., *Electrospinning for tissue engineering scaffolds.* Materials Science and Engineering: C, 2007. **27**(3): p. 504-509.

68. Kuddannaya, S., et al., *Surface Chemical Modification of Poly(dimethylsiloxane) for the Enhanced Adhesion and Proliferation of Mesenchymal Stem Cells.* ACS Applied Materials & Interfaces, 2013. **5**(19): p. 9777-9784.

69. Patel, N.G., et al., *Rapid cell sheet detachment using spin-coated pNIPAAm films retained on surfaces by an aminopropyltriethoxysilane network.* Acta Biomaterialia, 2012. **8**(7): p. 2559-2567.

70. Elineni, Kranthi K. and Nathan D. Gallant, *Regulation of Cell Adhesion Strength by Peripheral Focal Adhesion Distribution.* Biophysical Journal, 2011. **101**(12): p. 2903-2911.

71. Anderson, D.G., et al., *Biomaterial microarrays: rapid, microscale screening of polymer–cell interaction.* Biomaterials, 2005. **26**(23): p. 4892-4897.

72. Martino, S., et al., *Stem cell-biomaterial interactions for regenerative medicine.* Biotechnology Advances, 2012. **30**(1): p. 338-351.

73. Gilchrist, C.L., et al., *Micro-scale and meso-scale architectural cues cooperate and compete to direct aligned tissue formation.* Biomaterials, 2014. **35**(38): p. 10015-24.

74. Chou, L., et al., *Substratum surface topography alters cell shape and regulates fibronectin mRNA level, mRNA stability, secretion and assembly in human fibroblasts.* J Cell Sci, 1995. **108 (Pt 4)**: p. 1563-73.

75. van Dongen, S.F.M., et al., *Triggering Cell Adhesion, Migration or Shape Change with a Dynamic Surface Coating.* Advanced Materials, 2013. **25**(12): p. 1687-1691.

76. Heath, D.E., J.J. Lannutti, and S.L. Cooper, *Electrospun scaffold topography affects endothelial cell proliferation, metabolic activity, and morphology.* Journal of Biomedical Materials Research Part A, 2010. **94A**(4): p. 1195-1204.

77. Cavalcanti-Adam, E.A., et al., *Cell spreading and focal adhesion dynamics are regulated by spacing of integrin ligands.* Biophys J, 2007. **92**(8): p. 2964-74.

78. Chen, W., et al., *Nanotopography Influences Adhesion, Spreading, and Self-Renewal of Human Embryonic Stem Cells.* ACS Nano, 2012. **6**(5): p. 4094-4103.

79. Li, S., et al., *Protein adsorption and cell adhesion controlled by the surface chemistry of binary perfluoroalkyl/oligo(ethylene glycol) self-assembled monolayers.* Journal of Colloid and Interface Science, 2013. **402**(0): p. 284-290.

80. Kim, S.H., et al., *Correlation of proliferation, morphology and biological responses of fibroblasts on LDPE with different surface wettability.* J Biomater Sci Polym Ed, 2007. **18**(5): p. 609-22.

81. Yen, B.T., et al., *A comparison of the effects of fibre alignment of smooth and textured fibres in electrospun membranes on fibroblast cell adhesion.* Biomedical Materials, 2010. **5**(2): p. 025005.

82. Chen, M., et al., *Role of electrospun fibre diameter and corresponding specific surface area (SSA) on cell attachment.* Journal of Tissue Engineering and Regenerative Medicine, 2009. **3**(4): p. 269-279.

83. Charest, J.L., et al., *Combined microscale mechanical topography and chemical patterns on polymer cell culture substrates.* Biomaterials, 2006. **27**(11): p. 2487-2494.

84. Charest, J.L., et al., *Polymer cell culture substrates with combined nanotopographical patterns and micropatterned chemical domains.* Journal of Vacuum Science & Technology B, 2005. **23**(6): p. 3011-3014.

85. dos Santos, E.A., et al., *Chemical and topographical influence of hydroxyapatite and β-tricalcium phosphate surfaces on human osteoblastic cell behavior.* Journal of Biomedical Materials Research Part A, 2009. **89A**(2): p. 510-520.

86. Britland, S., et al., *Synergistic and Hierarchical Adhesive and Topographic Guidance of BHK Cells.* Experimental Cell Research, 1996. **228**(2): p. 313-325.

87. Britland, S., et al., *Morphogenetic guidance cues can interact synergistically and hierarchically in steering nerve cell growth*, in *EBO — Experimental Biology Online Annual 1996/97*. 1998, Springer Berlin Heidelberg. p. 15-34.

88. Ponche, A., M. Bigerelle, and K. Anselme, *Relative influence of surface topography and surface chemistry on cell response to bone implant materials. Part 1: Physico-chemical effects.* Proceedings of the Institution of Mechanical Engineers, Part H: Journal of Engineering in Medicine, 2010. **224**(12): p. 1471-1486.

89. Gallant, N.D., et al., *Micro- and Nano-Patterned Substrates to Manipulate Cell Adhesion.* Journal of Nanoscience and Nanotechnology, 2007. **7**(3): p. 803-807.

90. Wang, Y.C. and C.-C. Ho, *Micropatterning of proteins and mammalian cells on biomaterials.* The FASEB Journal, 2004.

91. Den Braber, E.T., et al., *Effect of parallel surface microgrooves and surface energy on cell growth.* Journal of Biomedical Materials Research, 1995. **29**(4): p. 511-518.

92. Lim, J.Y. and H.J. Donahue, *Cell sensing and response to micro- and nanostructured surfaces produced by chemical and topographic patterning.* Tissue Eng, 2007. **13**(8): p. 1879-91.

93. Shi, J., et al., *Incorporating Protein Gradient into Electrospun Nanofibers As Scaffolds for Tissue Engineering.* ACS Applied Materials & Interfaces, 2010. **2**(4): p. 1025-1030.

94. Ber, S., G. Torun Köse, and V. Hasırcı, *Bone tissue engineering on patterned collagen films: an in vitro study.* Biomaterials, 2005. **26**(14): p. 1977-1986.

95. Jin Ho, L., et al., *Interaction of fibroblasts on polycarbonate membrane surfaces with different micropore sizes and hydrophilicity.* Journal of Biomaterials Science, Polymer Edition, 1999. **10**(3): p. 283-294.

96. Hallab, N.J., et al., *Evaluation of metallic and polymeric biomaterial surface energy and surface roughness characteristics for directed cell adhesion.* Tissue Eng, 2001. **7**(1): p. 55-71.

97. Wirth, C., et al., *Biomaterial surface properties modulate in vitro rat calvaria osteoblasts response: Roughness and or chemistry?* Materials Science and Engineering: C, 2008. **28**(5–6): p. 990-1001.

98. Ponsonnet, L., et al., *Effect of surface topography and chemistry on adhesion, orientation and growth of fibroblasts on nickel–titanium substrates.* Materials Science and Engineering: C, 2002. **21**(1–2): p. 157-165.

99. Im, B.J., et al., *Texture direction of combined microgrooves and submicroscale topographies of titanium substrata influence adhesion, proliferation, and differentiation in human primary cells.* Archives of Oral Biology, 2012. **57**(7): p. 898-905.

100. Lee, S.W., et al., *Influence of microgroove dimension on cell behavior of human gingival fibroblasts cultured on titanium substrata.* Clin Oral Implants Res, 2009. **20**(1): p. 56-66.

101. Andersson, A.-S., et al., *Nanoscale features influence epithelial cell morphology and cytokine production.* Biomaterials, 2003. **24**(20): p. 3427-3436.

102. Cyster, L.A., et al., *The effect of surface chemistry and structure of titanium nitride (TiN) films on primary hippocampal cells.* Biomolecular Engineering, 2002. **19**(2–6): p. 171-175.

103. Cyster, L.A., et al., *The effect of surface chemistry and nanotopography of titanium nitride (TiN) films on primary hippocampal neurones.* Biomaterials, 2004. **25**(1): p. 97-107.

104. Akiyama, Y., et al., *Ultrathin Poly(N-isopropylacrylamide) Grafted Layer on Polystyrene Surfaces for Cell Adhesion/Detachment Control.* Langmuir, 2004. **20**(13): p. 5506-5511.

105. Mizutani, A., et al., *Preparation of thermoresponsive polymer brush surfaces and their interaction with cells.* Biomaterials, 2008. **29**(13): p. 2073-2081.

106. Lyu, S., et al., *Electrospun Fibers as a Scaffolding Platform for Bone Tissue Repair.* Journal of orthopaedic research : official publication of the Orthopaedic Research Society, 2013. **31**(9): p. 1382-1389.

107. Vogel, V. and M. Sheetz, *Local force and geometry sensing regulate cell functions.* Nat Rev Mol Cell Biol, 2006. **7**(4): p. 265-275.

108. Rumpler, M., et al., *The effect of geometry on three-dimensional tissue growth.* Journal of the Royal Society Interface, 2008. **5**(27): p. 1173-1180.

109. Rao, Y. and V. Haucke, *Membrane shaping by the Bin/amphiphysin/Rvs (BAR) domain protein superfamily.* Cellular and Molecular Life Sciences, 2011. **68**(24): p. 3983-3993.

110. Hsieh, W.-T., et al., *Curvature Sorting of Peripheral Proteins on Solid-Supported Wavy Membranes.* Langmuir, 2012. **28**(35): p. 12838-12843.

111. Itoh, T. and T. Takenawa, *Mechanisms of membrane deformation by lipid-binding domains.* Progress in Lipid Research, 2009. **48**(5): p. 298-305.

112. McMahon, H.T. and J.L. Gallop, *Membrane curvature and mechanisms of dynamic cell membrane remodelling.* Nature, 2005. **438**(7068): p. 590-596.

113. Fioretta, E.S., et al., *Differential Response of Endothelial and Endothelial Colony Forming Cells on Electrospun Scaffolds with Distinct Microfiber Diameters.* Biomacromolecules, 2014. **15**(3): p. 821-829.

114. Cheng, N. and X. Cao, *Photoactive SAM surface for control of cell attachment.* Journal of Colloid and Interface Science, 2010. **348**(1): p. 71-79.

115. Gallant, N.D., et al., *Micropatterned Surfaces to Engineer Focal Adhesions for Analysis of Cell Adhesion Strengthening.* Langmuir, 2002. **18**(14): p. 5579-5584.

116. Akintewe, O.O., et al., *Shape-changing hydrogel surfaces trigger rapid release of patterned tissue modules.* Acta Biomaterialia, 2015. **11**(0): p. 96-103.

117. Anselme, K., et al., *The interaction of cells and bacteria with surfaces structured at the nanometre scale.* Acta Biomaterialia, 2010. **6**(10): p. 3824-3846.

118. Brody, S., et al., *Characterizing nanoscale topography of the aortic heart valve basement membrane for tissue engineering heart valve scaffold design.* Tissue Eng, 2006. **12**(2): p. 413-21.

119. Karuri, N.W., et al., *Biological length scale topography enhances cell-substratum adhesion of human corneal epithelial cells.* Journal of Cell Science, 2004. **117**(15): p. 3153-3164.

120. Antipova, O. and J.P.R.O. Orgel, *In Situ D-periodic Molecular Structure of Type II Collagen.* Journal of Biological Chemistry, 2010. **285**(10): p. 7087-7096.

121. Hosseini, V., et al., *Fiber-Assisted Molding (FAM) of Surfaces with Tunable Curvature to Guide Cell Alignment and Complex Tissue Architecture.* Small, 2014. **10**(23): p. 4851-4857.

122. Ozdemir, T., et al., *Substrate curvature sensing through Myosin IIa upregulates early osteogenesis.* Integrative Biology, 2013. **5**(11): p. 1407-1416.